

UNIVERSIDAD POLITÉCNICA DE MADRID

**ESCUELA TÉCNICA SUPERIOR
DE INGENIEROS DE TELECOMUNICACIÓN**



**GRADO EN INGENIERÍA DE TECNOLOGÍAS Y
SERVICIOS DE TELECOMUNICACIÓN**

TRABAJO FIN DE GRADO

**STUDY, MODELLING AND DESIGN OF
INTERSATELLITE LINKS (ISL) IN MILLIMETER-WAVE
BAND**

**JOSÉ LUIS LASO FERNÁNDEZ
JULIO 2020**

TRABAJO DE FIN DE GRADO

Título: Estudio, modelado y diseño de enlaces intersatelitales (ISL) en bandas de milimétricas

Título (inglés): Study, modelling and design of intersatellite links (ISL) in millimeter-wave band

Autor: José Luis Laso Fernández

Tutor: Ramón Martínez Rodríguez-Osorio

Departamento: Departamento de Señales, Sistemas y Radiocomunicaciones

MIEMBROS DEL TRIBUNAL CALIFICADOR

Presidente: —

Vocal: —

Secretario: —

Suplente: —

FECHA DE LECTURA:

CALIFICACIÓN:

UNIVERSIDAD POLITÉCNICA DE MADRID

ESCUELA TÉCNICA SUPERIOR DE
INGENIEROS DE TELECOMUNICACIÓN

Departamento de Ingeniería de Sistemas Telemáticos
Grupo de Sistemas Inteligentes



TRABAJO FIN DE GRADO

**STUDY, MODELLING AND DESIGN OF
INTERSATELLITE LINKS (ISL) IN
MILLIMETER-WAVE BAND**

José Luis Laso Fernández

Julio 2020

Summary

The purpose of this Final Project is to explore the wide range of possibilities millimeter waves (and beyond) have to offer in their application to intersatellite links (ISL). Massive LEO constellations, such as OneWeb or Starlink, can benefit from millimeter waves technology, in terms of coverage, more robust global services or less need of ground stations. Therefore, multiple uses cases will be closely analysed and simulated in order to test it.

The goals that have been set are, first of all, to properly dimension the ISL using the millimeter waves frequency range. It includes the Link Budget calculation, using Adaptive Coding and Modulation (ACM). There, we shall obtain useful link indicators such as CNR, bit rate or total losses. Then, both transmitter and receiver schemes are set and specific electronic components from both ends of the ISL are proposed.

For this project I have worked with a space mission simulation software called FreeFlyer. The use of this type of tools simplifies greatly the design process of the use cases, and it offers multiple elements to analyse as well. From entire real constellations (such as OneWeb or Iridium), to the dynamic range estimation between two satellites or the possibility to calculate angles for a proposed beam in the transmitter. Once all the parameters have been calculated in FreeFlyer, they are exported to Matlab, where the Link Budget is estimated.

Resumen

El objetivo de este Trabajo de Fin de Grado es explorar las distintas posibilidades y oportunidades de uso que la banda de ondas milimétricas y superiores puede ofrecer en su aplicación para los enlaces intersatelitales (ISL). Interesa analizar con detalle distintos casos de uso y posibles escenarios de ISL utilizando tecnología de ondas milimétricas debido al incremento cada vez mayor de constelaciones LEO masivo como es el caso de OneWeb o StarLink y a las diversas ventajas que se obtienen, como puede ser conseguir una mejor conectividad y proporcionar unos servicios robustos de forma global o la necesidad de menos estaciones terrenas, entre otras.

Los objetivos que se han marcado son, en primer lugar, el dimensionado de los enlaces intersatelitales en milimétricas. Esto incluye el cálculo del Link Budget aplicando codificación adaptativa, obteniendo de manera dinámica parámetros como la CNR, tasa binaria o pérdidas de enlace; por otro lado, se proponen esquema de bloques y arquitectura de comunicaciones de los módulos transmisor y receptor del enlace, con una proposición de los componentes que los forman. Se podría plantear al final una comparación de la tecnología en ondas milimétricas con la tecnología óptica aplicada a dichos enlaces intersatelitales, para concluir cuál ofrecería mayores ventajas.

Para este Trabajo de Fin de Grado se han hecho uso de una herramienta software de análisis, diseño y simulación de misiones espaciales llamada FreeFlyer. El uso de este tipo de herramientas simplifica el proceso de diseño de los casos de uso planteados, además de ofrecer múltiples elementos para analizar, desde el diseño de constelaciones enteras, cálculo dinámico de distancias entre satélites o la posibilidad de insertar sensores con los que realizar estimaciones angulares en los enlaces. Por otra parte, se ha hecho uso del programa de cálculo Matlab, al que se han importado los resultados sacados de FreeFlyer para calcular el Link Budget, la tasa binaria o las pérdidas.

Key Words

Altitude, Adaptive Coding and Modulation, Argument of the Periapsis, Array, Array Factor, Azimuth, Bandwidth, Beamwidth, Bit Rate, BPSK, Constellation, Carrier to Noise Ratio, DVB-S, Eccentricity, Effective Isotropic Radiated Power, Elevation, Euler angles, Field of view, Formation, FreeFlyer, Frequency band, Gain, Gain fall, Gateway, GEO, Inclination, Intersatellite link, High Power Amplifier, Interplane, Intraplane, Iridium, LEO, Link Budget, Low Noise Amplifier, Massive LEO, MEO, Millimeter waves, Mixer, Noise Figure, Oscillator, OneWeb, Path loss, Payload, Phi, QAM, QPSK, Receiver, Right Ascension of the ascending node, Satellite, Sensor, Solid State Power Amplifier, Signal to Noise Ratio, Spacecraft, Starlink, Telesat, Theta, Transmitter, Travelling Wave Tubes Amplifier, 5G.

Acknowledgement

To my family and friends, that have given me the support to achieve my goals and have encouraged me to believe in my potential.

To Ramón Martínez Rodríguez-Osorio for supervising this project and orientating me throughout the whole process, which has not been easy due to the COVID-19 situation.

To AI Solutions Company, for providing me with a FreeFlyer student license that enabled me to do this project. It would not have been possible without it.

Contents

Summary	I
Resumen	II
Key Words	III
Acknowledgment	IV
Contents	V
1 Introduction, Motivation and Main Objectives	1
1.1 Introduction	1
1.2 Motivation	2
1.3 Main Objectives	3
1.3.1 Objectives	3
1.3.2 Document structure	4
2 Millimeter Waves	5
2.1 Why Millimeter waves	5
2.2 Use Cases	6
2.2.1 Biomedical Treatment	6
2.2.2 Intelligent Transportation Systems	7
2.2.3 High Speed Train Communications	8
2.2.4 5G	9
3 Satellite Communications, Massive LEO Constellations and ISL	11

3.1	Satellite communications	11
3.2	Massive LEO constellations	14
3.3	Intersatellite links	15
4	Simulation Design and Methodology	18
4.1	Introduction	18
4.2	Workflow	18
4.3	Simulation in FreeFlyer	20
4.3.1	Spacecraft, constellation and sensor design	20
4.3.2	Calculation of range, angular measurements and 2D or 3D visualization	21
4.3.2.1	Range	21
4.3.2.2	Angular measurements	22
4.3.2.3	Visualization	24
4.4	Simulation in Matlab	24
4.4.1	Data Import	24
4.4.2	Link Budget	24
4.4.2.1	Array antenna design	25
4.4.2.2	System temperature calculation	27
4.4.2.3	Adaptive Coding and Modulation (ACM) and link budget	28
5	Simulation Results	30
5.1	Introduction	30
5.2	Range	30
5.3	Angular measurement	31
5.4	Link Budget	34
5.4.1	Interorbital	34
5.4.2	Intraorbital	37

6 Payload Architecture	39
6.1 Introduction	39
6.2 Communication Payload	39
6.2.1 User link - ISL	40
6.2.2 Gateway link - ISL	41
6.2.3 ISL - ISL	41
6.2.4 User link - Gateway link	42
6.3 Component selection	42
7 Conclusions and future work	48
7.1 Conclusions	48
7.2 Future work	49
References	51
Appendix A Economic budget	i
A.1 Direct costs	i
A.1.1 Equipment Costs	i
A.1.2 License costs	i
A.1.3 Labour costs	ii
A.2 Project budget	iii
Appendix B Impact of this project	iv
B.1 Impact	iv
Appendix C Tables	vi
Appendix D FreeFlyer Code	ix
D.1 User guide	ix
D.1.1 Creating a constellation	ix

D.1.2	Propagating a satellite object	ix
D.1.3	Propagating a satellite in relation to another	ix
D.1.4	Configuring a sensor	x
D.1.5	Calculating range	x
D.1.6	Creating a VisibilitySegment	x
D.2	Range Measures	xi
D.3	Angular Measures	xi
Appendix E Matlab Code		xiv
E.1	Link budget code	xiv

List of Figures

1. Figure 1.1 Frequency Spectrum	1
2. Figure 1.2 LEO satellite system architecture	3
3. Figure 2.1 EH attenuation	6
4. Figure 2.2 LOS/NLOS comparison for 60 GHz indoor channel	6
5. Figure 2.3 S11 and S22 for different users	7
6. Figure 2.4 Automotive radars	8
7. Figure 2.5 High speed train mobile hotspot network for millimeter waves	9
8. Figure 3.1 Orbital parameters	12
9. Figure 3.2 Basic satellite communication diagram	13
10. Figure 3.3 Iridium constellation view with FreeFlyer	16
11. Figure 3.4 Iridium in a 2D map view with FreeFlyer	16
12. Figure 3.5 OneWeb constellation view with FreeFlyer	17
13. Figure 4.1 Methodology	19
14. Figure 4.2 FreeFlyer IDE	20
15. Figure 4.3 Theta and phi coordinates	23
16. Figure 4.4 Rectangular array antenna	25
17. Figure 4.5 Array placement	25
18. Figure 4.6 Noise temperature at the receiver	27
19. Figure 4.7 ACM scheme	29
20. Figure 5.1 Interorbital and intraorbital ISL range graphic in OneWeb	30
21. Figure 5.2 Interorbital sensor orientation	31
22. Figure 5.3 Euler angles system	31

23. Figure 5.4 Elevation/Azimuth Polar Plot	32
24. Figure 5.5 Alternative sensor orientation	33
25. Figure 5.6 Elevation/Azimuth Polar Plot for the new sensor orientation	33
26. Figure 5.7 Intraorbital sensor orientation	34
27. Figure 5.8 Gain fall graphic for a single element of the antenna	35
28. Figure 5.9 Interorbital Range-CNR graphic	36
29. Figure 5.10 Interorbital Time-Bit Rate graphic	36
30. Figure 5.11 Interorbital Range-Path Losses graphic	37
31. Figure 5.12 Intraorbital Time-Bit Rate graphic	38
32. Figure 6.1 Structure of the communication payload	40
33. Figure 6.2 User link - ISL architecture	40
34. Figure 6.3 Gateway link - ISL architecture	41
35. Figure 6.4 ISL - ISL architecture	42
36. Figure 6.5 User link - Gateway link architecture	42
37. Figure 6.6 ERZ-HPA-5000-6600-19	43
38. Figure 6.7 SFB-50375308-1519KF-N1	45
39. Figure 6.8 PE42525	46
40. Figure 6.9 IMUX	47
41. Figure 6.10 OMUX	47
42. Figure 7.1 Iridium range measures	49
43. Figure 7.2 GEO-LEO range measures	49

List of Tables

1. Table 1 Different LEO constellations	14
2. Table 2 Maximum θ and ϕ values relative to the field of view	32
3. Table 3 V band HPA/SSPA parameters	43
4. Table 4 V band Low Noise Amplifier parameters	44
5. Table 5 V band Mixer parameters	45
6. Table 6 V band Oscillator parameters	46

Introduction, Motivation and Main Objectives

1.1 Introduction

The boundaries of the telecommunication systems are about to be once again expanded, as technology is constantly improving and evolving. As new, exciting problems challenge the ICT sector, affecting every possible part of it (mobile communications, internet services, radar communications to biomedical applications or IoT) new solutions are also starting to emerge.

It does not come as a surprise that the overuse of the most commonly used frequency bands is starting to become one of these problems. Communications need to become faster, radio links are required to hold higher data throughputs and the demand for more robust services is notoriously increasing. This raises an obvious question: Is it suitable to adapt all these systems to higher frequency bands? What drawbacks and most importantly, what advantages may be found if doing so?

In this project, these questions will be analyzed for the millimeter-wave frequency bands.

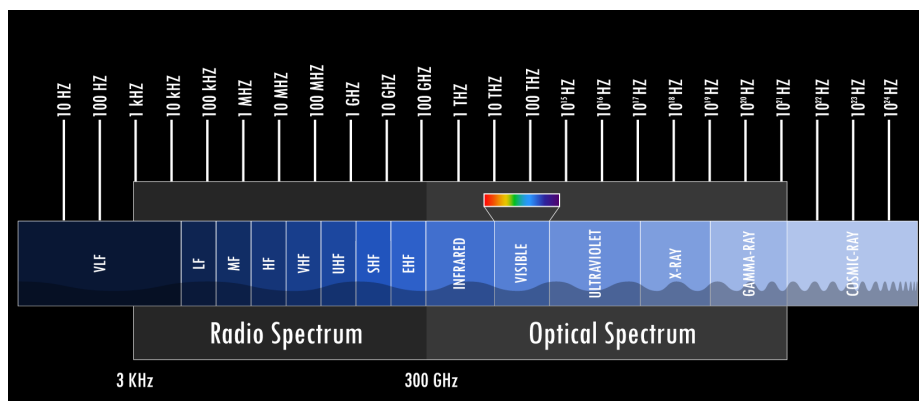


Figure 1.1 Frequency spectrum [1]

Millimeter waves are also referred to as Extremely High Frequencies (EHF) in the International Telecommunication Union (ITU) and correspond to the frequencies from 30 to 300 GHz. They were first used in a communications system when, in 1895, Sir Jagadish Chandra Bose demonstrated the feasibility of a 60GHz communication system where transmitter and receiver were separated 23 meters at Presidency College (Calcutta, India). Mr. Bose was able to remotely ring a bell and to detonate gunpowder using horn antennas, a spark transmitter, and dielectric lens, all within the constraints that his small laboratory had.

One of the main applications of millimeter waves is satellite communications, and more specifically intersatellite links (ISL). The first satellite to be ever launched was Sputnik I in 1957. Since then millions of them have been launched for various applications. The first ISL to be carried out in history was in 1975 by radio amateurs. The link was between AMSAT/OSCAR-7 and AMSTAR/OSCAR-6. OSCAR-7 received a signal at a frequency of 432.15 MHz and it was sent back to Earth at 145.95 MHz. On the other hand, OSCAR-6 received a signal at 29.50 MHz and was repeated to Earth. In this particular case, the ISL was extremely premature, hence it was available only when the satellites had a direct line of sight. Following this mission, NASA pursued testing of ISL between LEO satellites: ATSS-6 (April 1975), NIMBUS-6 (June 1975), Apollo-Soyuz Test Project (July 1975) to name a few.

However, these projects were working in lower frequency bands. The first satellites to ever use millimeter waves in ISL were the Lincoln Experimental Satellites 8 and 9, built at the MIT Lincoln Laboratory [2]. These two geosynchronous satellites were launched by NASA in 1976 under two approaches, millimeter waves and optical. For the millimeter waves link they established an ISL at 61.5 GHz, with a bit rate of 274 Mbps and 2 bits/symbol. The conclusions of the tests indicated that ISL millimeter waves technology was within reach and further research could be necessary in order to dig deeper into this kind of systems. However, the applications of millimeter wave ISL have been fundamentally experimental.

1.2 Motivation

Millimeter waves represent, along with massive Multiple Input Multiple Output (MIMO) and highly dense small cells, the key features that 5G will offer in terms of improvement. The growth of data demand makes it reasonable to look at EHF as one of the ways to obtain higher capacity, wireless broadband access and low latency uncompressed high definition media transfers. However, some issues remain to be completely covered, as these new systems are required to provide extremely good coverage, directionality and reliability, and that is not a trivial task.

Also, millimeter wave characteristics also pose challenges in terms of integrated circuits and system design, spatial reuse, interference management or path losses. They present much higher attenuation, specially at 60GHz due to the high oxygen absorption properties. This makes it possible to start considering new ways to build satellite communication systems and constellations, as millimeter waves can provide a better response to the great capacity demand of the future constellations that will be launched in the following years. They offer a higher reuse factor and therefore better employment of the spectrum compared to more conventional bands. Other than that, satellite payload is greatly affected by the use of millimeter waves in terms of size and weight. Therefore, intersatellite links are being greatly discussed lately due to new mega constellations that are starting to emerge, especially at LEO altitudes. This mega constellations enable users to have a significantly better coverage, if proper constellation diagrams are chosen. The intersatellite links should make it easier guarantee a quicker transmission of data, and fewer gateways would be needed in the ground segment and latency reduction thanks to the routing of the communication through the satellites of the constellation. Figure 1.2 shows an example of a LEO satellite communication system architecture. There it shown that intersatellite links might be able to connect gateways that are not in direct line of sight (LOS) with the same satellite.

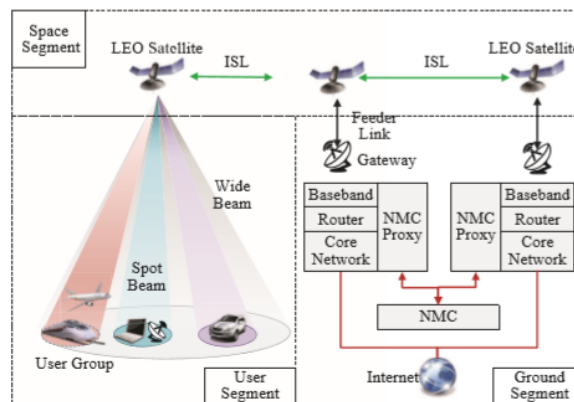


Figure 1.2 LEO satellite system architecture [3]

1.3 Main Objectives

1.3.1 Objectives

The goal of this project is to present what millimeter waves are, and to analyse the characteristics of this specific frequency band, in terms of attenuation, propagation, interference or noise. Then, various use cases will be mentioned and briefly examined, to showcase how

millimeter waves are causing a large number of areas to adapt and evolve, from biomedical devices or high speed train communications to radar and intelligent transport systems. Then inter-satellite links and massive LEO constellations will be introduced, and using FreeFlyer, a space mission simulation software tool, a use case scenario will be created to test the performance of millimeter waves for intersatellite links. A recreation of the OneWeb constellation will be created to make various calculations of range between satellite to be then exported to Matlab in order to make an estimation of the link budget, bit rate and total path losses for a proposed phased array antenna on both transmitter and receiver. A millimeter waves payload architecture will be also proposed.

1.3.2 Document structure

In this section we provide a brief overview of the chapters included in this document. The structure is as follows:

- **Chapter 2** Here millimeter waves will be analysed in more detail, as well as the main characteristics that make them interesting for further research. Also, a number of use cases will be mentioned and briefly analysed.
- **Chapter 3**: In this chapter the concept of intersatellite links will be fully explained, the application of millimeter waves in intersatellite links will be described in detail, and the importance of their use in the case of massive LEO constellations will be stated.
- **Chapter 4**: Once ISL and massive LEO constellations have been introduced, the methodology will be described, including the mathematical procedures, simulations and scripts executed in the different software tools to calculate all the graphics, tables and parameters that are needed to study the performance of millimeter waves, such as the Carrier-to-Noise-Ratio (CNR), the path losses, the bit rate or the performance of the Adaptive Coding and Modulation (ACM).
- **Chapter 5**: In this chapter the results of the simulation will be presented and analysed.
- **Chapter 6**: Here the payload structure will be presented, along with the general scheme for both the transmitter and receiver modules, and commercial millimeter waves components with their fundamental parameters such as gain or noise figure.
- **Chapter 7**: Finally, the following conclusions will be made and future research lines will be set.

Millimeter Waves

2.1 Why Millimeter waves

The ITU defines millimeter waves, or Extremely High Frequency, as the frequency band from 30 to 300 GHz, or 10 to 1 mm. Currently, their main applications include satellite Earth exploration (both fixed and mobile), space research, radionavigation, radiolocation, mobile communications, broadcasting, defense or amateur satellite communications.

Thanks to the wide bandwidth available (multiple GHz), millimeter wave services can achieve high throughputs, multi-Gigabit/s transmissions. Also, due to the small wavelength, antennas can become significantly smaller if properly designed, without any significant trade-offs, making it feasible to condensate signals in highly focused beams, to gain directivity. As 5G arrives (it is estimated that around 1.01 billion 5G connections will exist by 2023 [4]), this will help to use millimeter wave antennas into almost any device ensuring high data rate and integration.

One of the most important characteristics of millimeter waves is their propagation behavior. They mainly propagate in LOS paths and gaseous attenuation plays a big role in the transmission losses term, especially around 24-30 GHz and 60GHz where water vapor and oxygen respectively cause local absorption peaks that exceed the usual free space losses (Figure 2.1). Millimeter waves do not generally propagate well in long-range transmissions. This makes it easier for communication design to have a higher frequency reuse factor, and therefore make more efficient use of the spectrum and the amount of interference between near transmissions [5]. Also, bad long-range propagation characteristics make millimeter waves extremely good in ensuring security and isolation in short-range (less than 1 km) communication transmissions, hence they are suitable for highly dense communication networks.

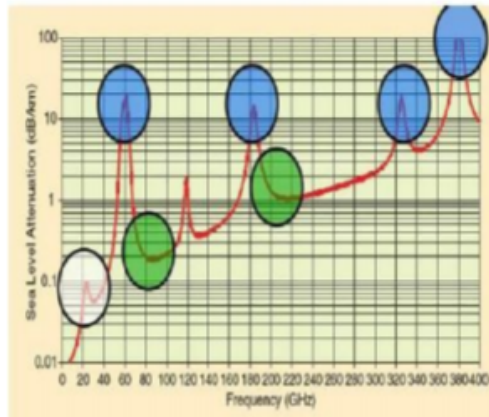


Figure 2.1 EHF attenuation [6]

The 60 GHz peculiar absorption peak than oxygen molecules make has increased the interest for researchers and engineers on that section of the EHF spectrum. It is known that free space losses at 60GHz are around 30 dB greater than at 2 dB for a signal of wavelength of 5mm. The attenuation caused by the oxygen goes from 15 to 30 dB/km there. It is also clear, from what many pieces of research indicate, that LOS paths suffer less attenuation than NLOS, as Figure 2.2 shows for an indoor path channel measurement.

$PL(d_0)$ [dB]	n		σ [dB]
Corridor	68	1.64	2.55
LOS hall	682.17	0.88	
NLOS hall	68	3.01	1.55

Figure 2.2 LOS/NLOS comparison for 60 GHz indoor channel [6]

2.2 Use Cases

Following the description and characteristics of millimeter waves there are a number of use cases that will be briefly presented.

2.2.1 Biomedical Treatment

Millimeter waves have been recently applied for biometric individual identification. Biometric systems, have the task of verifying the identity offering an identification method that is less dependant on physical keys or passwords. Traditional identification strategies as these two are based normally on things we know: numbers, dates, names, Personal Identification

Numbers..., These can be easily lost or stolen. Biometric identification systems will be the new strategy in the near future, and most of them will involve physiological features: Faces, fingerprints (Automated Fingerprint Identification Systems), iris, retina, voice... However, it seems feasible for criminals to hack most of these methods as well, for instance, fingerprint or hand signatures. Other methods are more reliable but are more invasive for the user, especially the optical-based identification systems.

Therefore other solutions have been proposed. In the University of Waterloo in Canada, a prototype system was proposed in 2017 for the biometric identification of users using palmprints. Millimeter waves have a great advantage here due to their propagation properties at 60GHz. The human skin has three different layers of different thickness: the epidermis (from 0.5 mm to 1.5 mm), dermis (from 0.6 mm to 3 mm), and subcutaneous tissue (variable depending on the amount of fat accumulated). Therefore millimeter waves with a wavelength of 5 mm at 60GHz present good conditions to be used for identification.

They used an 8 channel (2 transmitters and 4 receivers) monostatic radar with a frequency-modulated continuous wave operating in the 57-64 GHz frequency band, integrated into a flat plate. Two horn antennas are situated at a distance of 6 mm from the surface. The system uses the scattering parameters to distinguish and identify users, as they were clearly different depending on the user as Figure 2.3 illustrates.

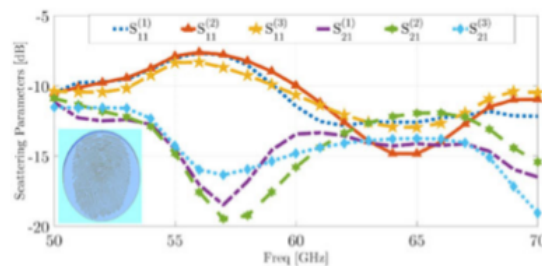


Figure 2.3 S11 and S22 for different users [7]

2.2.2 Intelligent Transportation Systems

Intelligent transportation systems use technology to improve traffic management and the user's knowledge of what the conditions are, and making sure that the transport systems become safer and smarter.

Radars play a significant role in ITS. Automotive radars are a key factor in the near future automotive industry, as they are used for pre-collision detection, airbag boosting, blind spot detection, parking assistance, and back drive assistance. They are divided into

two groups: long range radars and short range radars. Millimeter waves are normally used for short range radars, due to their propagation properties.

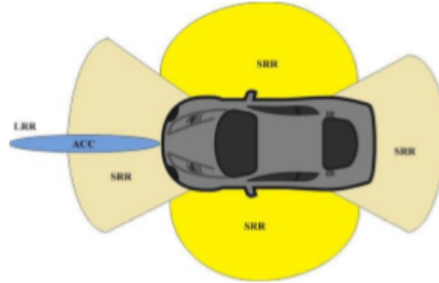


Figure 2.4 Automotive radars [8]

Also, Vehicle-to-Vehicle (or intervehicle) and Vehicle-to-Internet (or roadside-to-vehicle) wireless millimeter wave communications have been carefully studied. Thanks to the oxygen absorption at 60GHz, its poor penetration properties, and the little influence that the Doppler effect has on them, it is reasonable to propose this kind of systems.

In the case of Vehicle-to-Vehicle, real time data is shared, within the ranges that millimeter waves are able to transmit information, between different vehicles, and bad weather conditions have no significant effects on the communication links. Again, thanks to the properties of millimeter waves, antennas can be significantly reduced in size and easily integrated into the structure of cars.

Vehicle-to-Internet communications involve roadside infrastructure to connect the vehicles to the net, and it is normally used for instant recognition of objects, faces, and gestures.

2.2.3 High Speed Train Communications

Millimeter waves mobile networks have been proposed for high speed train communications in the Seoul subway system. Due to the significant increase of mobile data traffic from smartphones, in particular, the interest in developing a system that supports the users connection at every moment is growing greatly, as this would enable the user to connect to the net not only at home or at work, but also on the various means of transportation. But it is quite frequent to experience poor quality connections or connection failures when connecting to the current Wi Fi onboard systems, due to limited capacity.

This system was based on the creation of a number of mobile hotspots connected to networks. Users would be able to connect to these hotspots via Wi Fi.

Millimeter waves are used here due to their good properties in LOS communications

(channel measurements were made and the delay spread was less than 10 ns). There were a number of problems that were addressed, high attenuation losses due to the absorption peaks at some frequencies, a high Doppler effect due to fast variations of the transmission link over time, the geometry of the tunnels (the delay spread in NLOS channels was around 32.1 ns), or frequent handovers between trackside antennas due to the speed of the trains in motion (this causes a reduction in the average data rate).

For the design of the system that was proposed, 32 GHz was selected as the carrier frequency, and a bandwidth of 250 MHz split in two bands of 125 MHz was used. The user would connect to each hotspot via Wi Fi and the data slots would consist of radioframes of 10 ms split into 5 subframes of 8 slots, each of those subframes would have a duration of 250 μ s. Each slot would contain 40 OFDM symbols. Each backhaul link would consist of an 8x8 patch array antenna with a gain of 22 dBi, as Figure 2.5 shows.

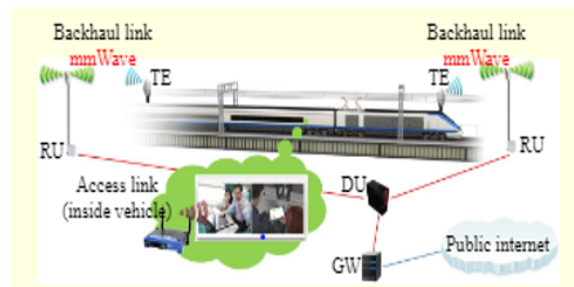


Figure 2.5 High speed train mobile hotspot network for millimeter waves [9]

After various simulations, it was concluded that a beamforming strategy for both the transmitter and the receiver was the most convenient choice. The highest data throughput that was achieved during those simulations was 500 Mbps, which was significantly higher than the average data rate available in the previous system. Overall, the results of the simulations were positive and the application of millimeter waves to high speed train connections was proved to be a suitable option.

2.2.4 5G

As previously mentioned, millimeter waves are one of the three main axis of the next radio interface of 5G, along with massive MIMO and densification.

5G is yet to be completely defined, but the main goal that is pursuing is to obtain a higher capacity and less cost, making more efficient use of the spectrum and using higher frequency bands. The idea of using small cell densification and multi-layer deployment, along with OFDM and MIMO techniques, does not provide a good solution on its own,

as co-tier interference between adjacent cells is still taking place. Therefore densification and MIMO must be complemented with techniques that are able to take advantage of the great amount of bandwidth that is still being left unexploited, and at the same time to fight against interference from other cells. This is where the interest in millimeter waves appears. They offer the potential use of a large number of GHz of spectrum for mobile communications, and the use of higher frequencies makes it possible for terminals to have a reasonable size (antennas at 30 GHz have a size of approximately 10mm, and of 5mm at 60GHz). Also, millimeter wave communication cells are reduced in size (around 200m), which, according to researchers, will make rain and atmospheric absorption less harmful for transmission.

However, there are still a number of issues that remain unclear, especially in terms of propagation, as millimeter wave characteristics make the transmission of signals less reliable and NLOS channels have a greater impact than at lower frequencies. However, beamforming techniques are being proposed to provide directivity in order to mitigate the propagation effects.

Despite all the research done around this matter, there is still work to be done for a complete characterization of the millimeter wave contribution to 5G. Adapting the radio interface to this new technology will certainly be the greatest challenge ahead.

Satellite Communications, Massive LEO Constellations and ISL

3.1 Satellite communications

Satellite communications constitute a fundamental part of the telecommunication and broadcast of a wide variety of services since their use began.

Their main characteristics are:

- Multiple access: Point-to-point, point-to-multipoint or multipoint-to-multipoint connectivity.
- Distribution in point-to-multipoint transmissions (including multimedia broadcasting and data transmission).
- Flexibility and adaptability.

They normally consist of a space segment and a ground segment. The space segment is where the satellite is located as the core element of the system. These satellites communicate thanks to the different transponders they have, which can be transparent (also known as repeaters, they just receive transmissions and resend them after amplification and frequency operations) or on-board processing transponders or OBP (these can perform frequency/time/space switching, regeneration of the signal and baseband processing).

Satellite orbits can be classified in many ways, one of the most common ones is depending on their distance to the Earth:

- Geostationary orbit (GEO): They have an altitude of around 36000 km and are normally used for communication, navigation or meteorology purposes. Due to their orbit characteristics, they seem stationary, and do not require of movable antennas on the ground segment. Their orbital period is 24 hours and they are not good for small

terminals. They have permanent visibility from the ground segment.

- Medium Earth orbit (MEO): They are situated between the GEO and LEO satellites, and are commonly used as navigation systems (Galileo), or communication systems like the O3B system that provides voice and data communications, specially in remote locations where broadband Internet is not available. Their orbital period is from 5 to 12 hours. They have a visibility period from the ground segment of 8 hours per pass.
- Low Earth orbit (LEO): They have an altitude of 2000 km or less. Satellites at these orbits have a reduced field of view. Therefore when referring to LEO satellites it not casual to talk about satellite constellations, as it is the way to guarantee continuous coverage. The average visibility period here is between 15 and 20 minutes per pass.

Orbits are normally ellipses that are characterized by a number of parameters, as it is shown in Figure 3.1. The most important of them are:

- Argument of periaapsis (ω): It is an angular indicator that defines how the ellipse is oriented in the orbital plane.
- Altitude (A): The distance from the surface of the Earth. When adding the radius of the Earth we have the total radius of the orbit.
- Eccentricity (E): It describes how "circular" the orbit is. When it is equal to 0 the orbit is circular.
- Right ascension of the ascending node or longitude of the ascending node (RAAN): Angular indicator of the orbit with respect to the reference plane (Parallel to the Equator).
- Inclination (I): Vertical angular indicator with respect to the reference plane. An inclination of 0° means that the orbit is basically always at the latitude of the Equator.

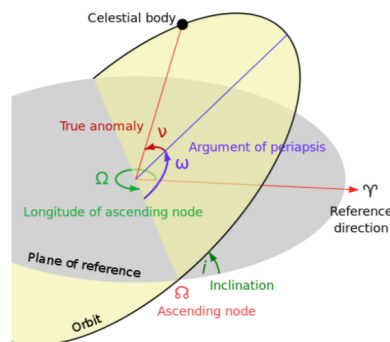


Figure 3.1 Orbital parameters [10]

Basic satellite links, normally consist of a duplex communication channel between Earth stations and a satellite. The simplest case is composed of two earth stations and a transponder (or a number of them) as shown in Figure 3.2. As previously mentioned, the satellite can simply repeat the signal after some amplification and frequency maneuvers, or it can perform more complex operations in the case of OBP.

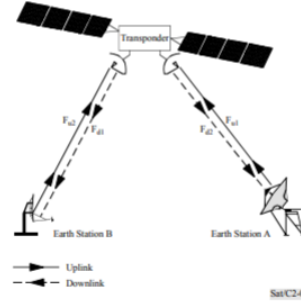


Figure 3.2 Basic satellite communication diagram [11]

Thus, satellite communications depend on the reliability of the links that are established. The carrier to noise ratio is the main indicator of whether the link is in good transmission conditions or not. Equation 3.1 describes the way to calculate the carrier to noise ratio concerning the transmitter, propagation losses, and receiver characteristics (bandwidth, the temperature of the receiver, gain).

$$C/N(dB) = EIRP + G/T - L_t - 10\log(kB) \quad (3.1)$$

Equations 3.2 and 3.3 describe the formulas of the noise temperature of the system (including the antenna) and the receiver (g_1, g_2, \dots, g_{n-1} , represent the total gain of each module in the receiver).

$$T(K) = T_a + T_{rx} \quad (3.2)$$

$$T_{rx}(K) = T_1 + T_2/g_1 + T_3/(g_1g_2) + \dots + T_n/(g_1g_2 \dots g_{n-1}) \quad (3.3)$$

Equations 3.4 and 3.5 represent the total path losses (including pointing (L_{ap}) and polarization (L_{pol}) losses and the losses at the transmitter (L_{tx}) and receiver (L_{rx}) respectively, mainly coupling losses) and the free space propagation losses L_{bf} (d is the total distance of the link and λ is the wavelength of the signal)

$$L_t(dB) = L_{bf} + L_{ap} + L_{pol} + L_{tx} + L_{rx} \quad (3.4)$$

$$L_{bf}(dB) = 20\log(4\pi d/\lambda) \quad (3.5)$$

Equation 3.6 describes the Effective Isotropic Radiated Power or EIRP, that includes the transmitted power and the gain of the transmitting antenna.

$$EIRP(dB) = P_{tx} + G_{tx} \quad (3.6)$$

These are the main formulas for the estimation of a link budget in satellite communications, whether it is an uplink from the Earth station to the satellite, a downlink back to Earth, or an intersatellite link.

3.2 Massive LEO constellations

LEO orbits are very commonly used in satellite communications. They normally serve the purpose of providing a connection to a large number of terminals. They do not need to follow specific paths around the planet, like GEO satellites do, and impose less general restrictions. Delays are greatly reduced in these constellations (time between two earth stations via satellite at a distance of 1000 km from Earth is less than 10 ms approximately). Some examples of LEO constellations are shown below in Table 1:

LEO constellations				
Name	N.satellites	Orbital planes	Altitude (km)	Frequency band
OneWeb	720	18	1200	Ku (users) Ka (gateways)
OneWeb (After extension)	1980	36	1200	Ku (users) Ka (gateways)
Starlink	4425	83	550	Ku (users) Ka (gateways)
Telesat	117	11 (6 polar and 5 inclined)	1000-1200	Ka (users) optical (ISL)

Table 1 Different LEO constellations

LEO satellite network systems are normally based on small cells. Therefore a user terminal will connect with a satellite that is visible from the cell. From the satellite, the

information will be transmitted again, either through intersatellite links or directly, back to Earth.

Network management techniques in LEO constellations are key to provide the user with continuous connection regardless of the specific satellite that is in LOS with the ground segment. Due to the small field of view of the satellite, a given cell is not receiving the same beam permanently but is regularly switching from one beam to another from a different satellite. Therefore, soft call handover techniques are used in the entire system (both the ground and space segments) to ensure continuous communication.

Their power requirements normally go from 0.5kW to 3kW, which will partly determine the size of the satellite. This is generally lower than in GEO or in MEO, due to a shorter range of transmission. They normally use either reflectors or phased arrays as antennas, or a combination of both. Arrays are more used in LEO. Normally, a multibeam approach is used to obtain higher EIRP and G/T as well as reducing the requirements in the ground terminals. This leads to small sized beams and bigger antennas. Array antennas in LEO satellites are intended to be reconfigurable in order to dynamically point to different areas at their convenience, as it occurs in constellations like Iridium.

Millimeter waves are being linked to satellite communications lately. As 5G arrives, and the radiocommunication channels demand higher capacity and reliability, researches and projects are starting to look at higher frequency bands for new opportunities. The millimeter wave band, between 30 and 300 GHz seems like a reasonable choice when making new proposals for satellite systems, as they can provide a wide band of spectrum.

3.3 Intersatellite links

Intersatellite links (ISL) are the main topic of discussion in this project. They serve as communication channels between two satellites and can be classified into three different categories:

- LEO-to-LEO
- LEO-to-GEO
- GEO-to-GEO

In terms of constellation schemes, the Walker patterns seem to be one of the most reasonable choices. There are two main variants: the Walker Delta pattern and the Walker Star pattern. The Walker Star differentiates from the Delta in that it presents near-polar orbits that spread in a 180° range around the globe, while the Delta are not near-polar

orbit. This makes the Walker Star model a more suitable scheme for ISL, as the relative position between satellites from adjacent planes does not vary as in other models like the Delta pattern. For multiple access, FDMA and TDMA are normally employed techniques. Normally phase shifting key modulations are used in digital satellite communications, including ISL, specially BPSK and QPSK. As mentioned previously in Equations 3.4 and 3.5 ISLs present propagation losses that include free space propagation, pointing, polarization, and coupling losses. As there is the very little atmospheric effect for the most part of ISL it does not represent a significant loss in the link budget. However, there are some difficulties to be taken into account when designing a ISL as the need to accurately track the other satellite, because the two ends of the ISL will be in constant propagation in their own orbits, therefore continuous pointing will be crucial to achieve a good communication channel or the demand for high gains on both ends of the links due to low power levels.

Here two examples of LEO satellite constellations will be presented. One of them (Iridium) uses ISL, the other (OneWeb) does not use them, and their constellation parameters will be used as simulation scenarios in Chapters 4 and 5:

- Iridium: The Iridium satellite system was originated in 1987 at the Satellite Communications Division of Motorola. It is composed of 66 satellites in 6 LEO orbit planes (11 satellites per plane). Each plane has an inclination of 86.4° and satellites in the plane have a constant spacing between them of 32.7° .

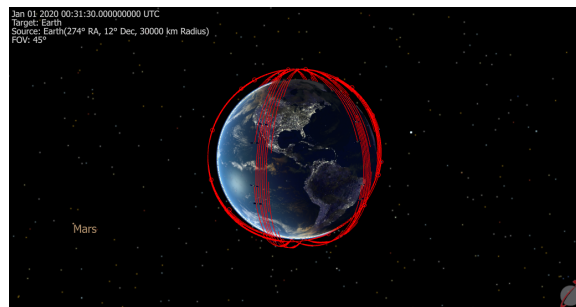


Figure 3.3 Iridium constellation view with FreeFlyer

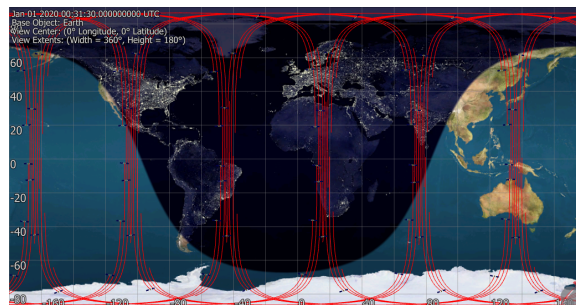


Figure 3.4 Iridium in a 2D map view with FreeFlyer

Each Iridium satellite presents a duplex link with the ground segment and also has

four ISL except for satellites in counter-rotating planes one and six, where they have 3 ISL due to the quick angular change between them. They both operate in the Ka band (ISL operate between 22.55 and 23.55 GHz) and use circular polarization. TDMA and FDMA combination is used for multiple access.

- OneWeb: The OneWeb satellite system initially has 720 satellites in 18 polar planes (40 satellites per plane) situated at a distance of 1200 km. Each plane has an inclination of 86.4° . User links are in Ku band and gateway links are in Ka band. ISL are not implemented.

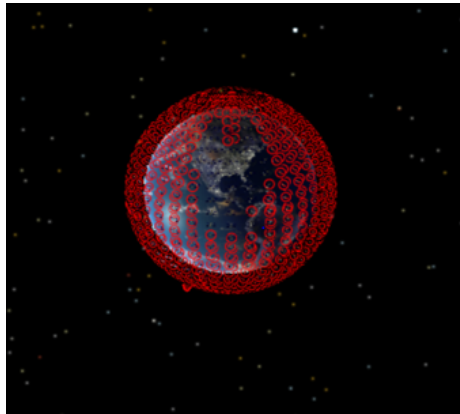


Figure 3.5 OneWeb constellation view with FreeFlyer

The estimated maximum throughput that OneWeb can provide is around 1.56 Tbps with 71 ground stations [12]. It is considered that ground segment terminals could be significantly reduced if OneWeb used ISL

Simulation Design and Methodology

4.1 Introduction

In this chapter, the design of this project will be presented, as well as details involving the simulation in the FreeFlyer software and in Matlab. Firstly, we present an overview of the project, divided into several modules to offer the reader a general view of the procedure. Then, each module will be presented separately in much more depth.

4.2 Workflow

In order to analyse the performance of millimeter waves in intersatellite links, we will follow the procedure described in Figure 4.1. First of all one use case will be selected from a set of possible scenarios:

- Iridium ISL
- OneWeb ISL
- GEO-LEO ISL

In this project we will analyse in close detail the OneWeb ISL use case. OneWeb is of particular interest as a case of study as it has ISL as one possible addition to its future generations of satellites. Once the use case has been chosen, using the FreeFlyer scripting language, these scenarios will be created. Thanks to the wide range of options and tools that this simulation software offers, we will be able to create full satellite constellations, single satellites, sensors, and to edit multiple parameters when declaring any of these FreeFlyer objects. Then we will proceed to calculate dynamically (1) the distance between specific satellites from the same constellation (both intraplane and interplane satellites) or from different orbit types (in the GEO-LEO scenario), (2) angular measures in order to design the antennas and beam steering procedures in the ISL, (3) the number of satellites that fit

into the field of view and (4) will display 2D and 3D visualizations and graphics.

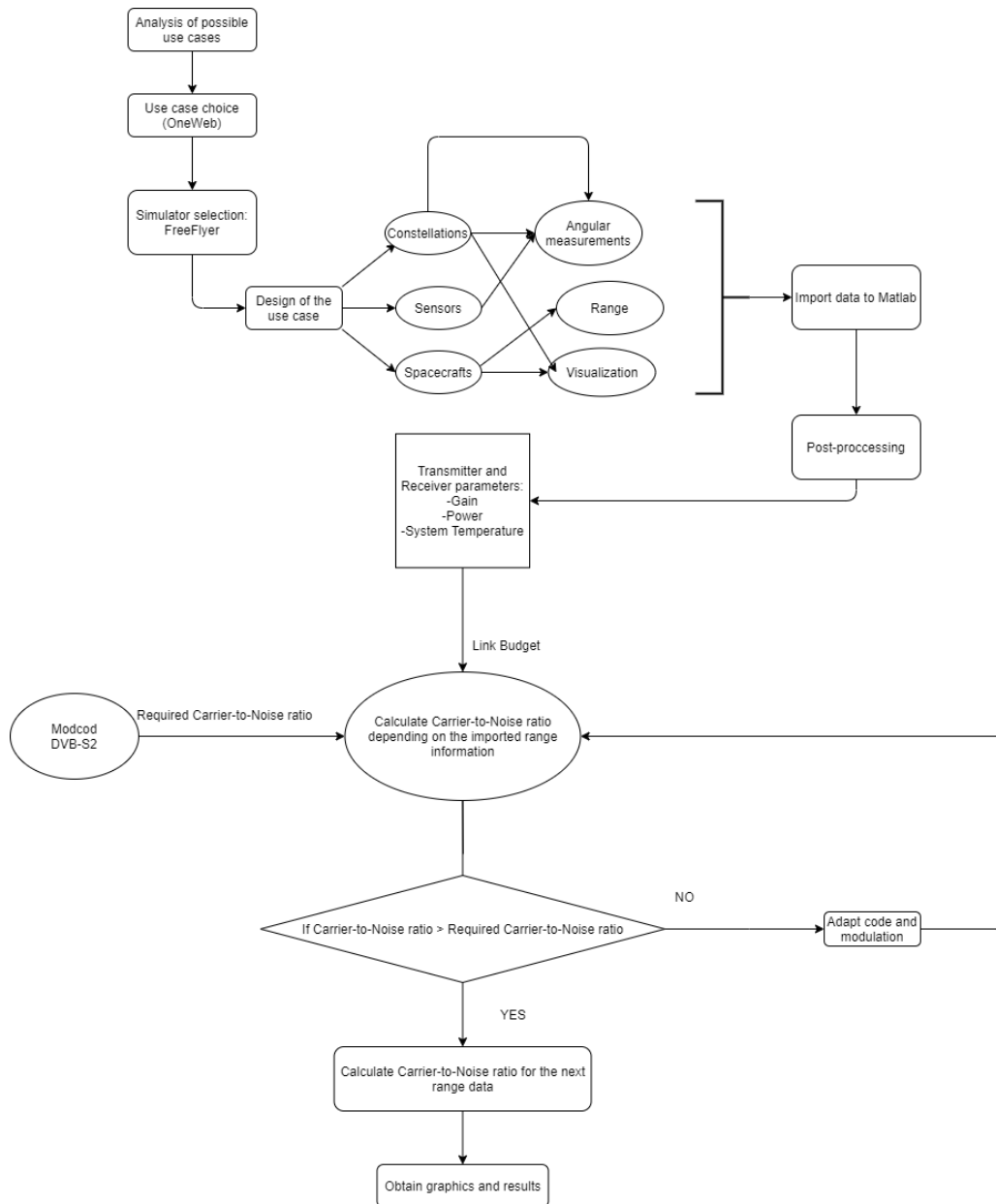


Figure 4.1 Methodology

After all the data has been generated, it will be exported to Matlab, to be used for the calculation of the link budget. Before actually calculating the link budget some parameters have to be defined. In both receiver and transmitter the gain is set based on the design of the antenna. For this project, we have chosen a bidimensional phased array antenna with uniform amplitude. Additionally the noise temperature will be estimated based on the architecture of the ISL payload. Only once all the parameters have been established the

link budget will be calculated. For this we will apply an Adaptive Coding and Modulation (ACM) technique to dynamically adapt the bit rate depending on the propagation conditions and losses. We used a MODulation and CODing (MODCOD) scheme that could adapt to multiple standards. After calculating the CNR the results will be analysed in Chapter 5. We will go into depth on each of the different stages of this workflow that has been exposed.

4.3 Simulation in FreeFlyer

FreeFlyer is a commercial software created by AI Solutions for space mission simulation, design and analysis. For this project, AI Solutions provided us with a full academic FreeFlyer license in order to take advantage of its potential to create the different scenarios. Code examples of the FreeFlyer simulation will be added in Appendix D.

4.3.1 Spacecraft, constellation and sensor design

FreeFlyer works under its own native scripting programming language. It offers a wide range of options from 2D and 3D visualization, sensor modeling, satellite modeling, constellation modeling, plotting, and orbit and space environment modeling. There are a number of objects that can be added and edited within the FreeFlyer simulator, such as: Spacecrafts, Formations, Sensors, Vectors, Ground Vehicles, Ground Stations and many others. Once we have selected the scenario to simulate and analyse we must create it in FreeFlyer. To do that we must add either a "Spacecraft" or a "Formation" (depending on what scenario we want to create, "Spacecraft" corresponds to a single satellite and "Formation" to an entire satellite constellation). For example if we want to create a constellation we must first add a Formation object to the Object Browser as Figure 4.2 shows.

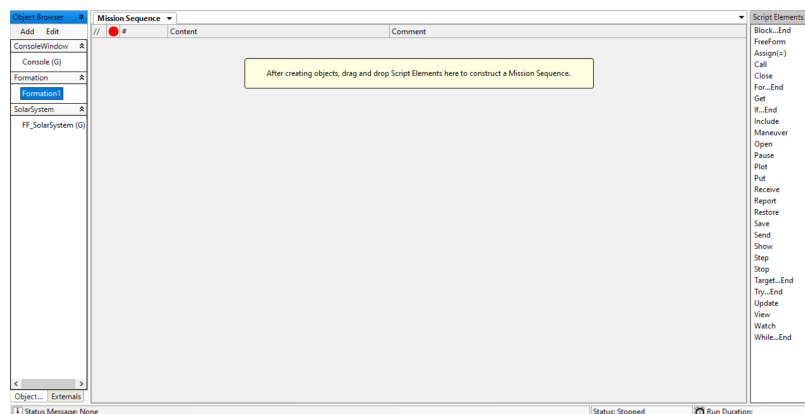


Figure 4.2 FreeFlyer IDE

Then we must insert its orbital parameters inside two *for* loops (i separates orbital planes and t separates satellites from the same orbital plane) where each satellite in the constellation will acquire its own orbital parameters (A = Altitude, I = Inclination, RAAN = Right Ascension of the Ascending Node, W = Argument of the Periapsis). When defining the W parameter we must also define the relative phase shift parameter. It adds an extra angular value to the W parameter to make sure that satellites do not collide at the point where their trajectories intersect. To create a single satellite is a simpler process, as it is equivalent to create a single member of a constellation. It will have to be added to the Object Browser as a "Spacecraft". In the case of single satellites, FreeFlyer offers the Orbit Wizard interface to edit all the orbital parameters in a quicker way.

After having created either a constellation or a single satellite, if we want them to propagate their orbit (this will be necessary to dynamically calculate the range) we must use the *Step* command inside of a *While* loop. If we want to propagate more than one satellite we must first use the *Step* command for the first one as previously indicated, and then use it for the second one with respect to the time span of the first. In the case of constellations, a single *Step* command is enough.

A sensor will be added in our use case scenario to obtain angular measures for the design of the array antenna. It can both be done with a script or by editing the properties of spacecraft where the sensor is going to be placed, but for constellations it is easier to do it via script. It is simply done by the *.AddSensor()* command. We will be asked to name it (*sensor1*). Through the *ConeHalfAngle*, *ZAxisAzimuth* and *ZAxisElevation* the orientation and field of view will be defined. In order to do this we must set the *ViewAsGroup* property of the constellation to 0, otherwise FreeFlyer will not let the user add sensors to any of the satellite members of the constellation.

4.3.2 Calculation of range, angular measurements and 2D or 3D visualization

4.3.2.1 Range

In order to calculate the link budget for an ISL one of the fundamental parameters to calculate is the distance between the two satellites. As (3.5) indicates, free space propagation losses are directly dependant on distance from the transmitter to the receiver. We will make a distinction between intraorbital and interorbital ISLs. Intraorbital ISL corresponds to satellites that belong to the same orbital plane. If that is the case, the range should have a relatively constant value. If it is an interorbital ISL the range should have an obvious variation, as the satellites will approach and drift away at different points during their

orbital trajectory.

When declaring a constellation or a satellite in FreeFlyer we must choose the orbital propagator or Integrator type, as it is called in FreeFlyer. Orbital propagators or Integrators in FreeFlyer define what force model and step properties are going to influence our satellites when performing a simulation. There are a few Integrators to choose from: Runge Kutta 8(9), Runge Kutta 4(5), Runge Kutta 7(8), Bulirsch Stoer, Cowell, Norad, J2Mean or Two-Body are some of them. For our study the Two-Body Integrator type has been chosen, as it offers high computational speed and a relatively good accuracy for our standards. It is based on the Kepler laws, assuming that the mass of the satellite is negligible in comparison to the mass of the Earth, they present uniform density and are spherically symmetrical, which makes it possible to reduce them to points of mass. We also assume that the only forces that influence both the Earth and the satellite are the gravitational forces that attract the two points of mass. With the Two-Body Integrator the distance in intraorbital ISLs should be literally constant.

FreeFlyer can calculate the distance between two different spacecrafts thanks to a command called *Range*, which will return a numerical value (in kilometers by default). This would be done by invoking this command on one satellite in the constellation in relation to the other.

In our use case it is useful to define what it is referred as a *VisibilitySegment* in FreeFlyer, as direct ISLs are not feasible when there is no LOS between the ends of the communication channel. In order to do this we must set both the *Observer* or Transmitter and the *Target* or Receiver. It also needs to be defined what the obstacle that does not enable the visibility is. For the most part, it is the Earth itself that is placed in between two satellites, that will be declared with the *AddOccludingBody* property, and with the *CelestialObjectOccultationModel* property set to 0 we will be able to define the Earth body as a sphere. Thus, we will have to let FreeFlyer know that a range calculation will be only necessary when the *Observer* and the *Target* are in LOS. This will be done through the *Visibility* command, that will return a 1 value if the *VisibilitySegment* is in LOS.

4.3.2.2 Angular measurements

In the design of the array antennas, it will be necessary to establish the angular range that the array will cover, in both *theta* and *phi* angular coordinates. In order to do this, a sensor object has been used in order to get the number of satellites that are within its field of view as well as to calculate the angular measurements for each of those satellites. A sensor

can serve as a simplified version of a beam in the case of satellites in FreeFlyer. It offers different options both for the orientation (Euler Angles, Unit Vector, Azimuth-Elevation,...) and shape (Cone, Rectangle or Custome Shape) setting of the sensor. In our case the Euler Angles option and the cone shape have been selected.

The antenna would be placed in the XY plane, which will be one of the multiple sides of the satellites. The Z-axis of our sensor will define the *theta* and *phi* angular coordinates, as it is shown in Figure 4.3:

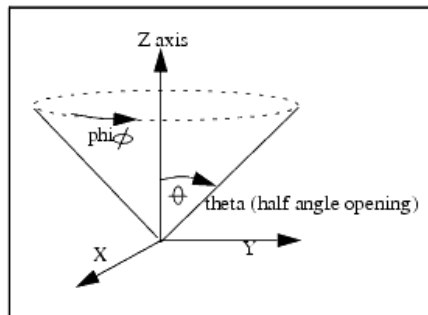


Figure 4.3 Theta and phi coordinates

Interplane ISLs are normally set between adjacent orbital planes. It is intended to orientate the sensor to include in its field of view as many satellites as it can, and then to obtain the angular values of those satellites. Through the *.BoresightRotationSeq* and *.BoresightAngles* commands, the sensor will be orientated in whatever way we want to. Once the sensor has been set the procedure to obtain the angular measures will be as follows. Firstly we will create a list of *VisibilitySegment* elements, in which the sensor will be the Observer and the satellites will be the Targets, with the exception of the one where the sensor is placed.

For a given constellation, using a *for* loop, the number of satellites that are visible for the sensor will be calculated, which will let us define the size of two array objects where the values for the theta and phi measures will be stored. Then, inside another *for* loop, thanks to the *.Elevation* (theta) and *.Azimuth* (phi) commands we will be able to obtain directly these two values for each of the satellites that are situated within the field of view. The full script will be included in Appendix D. The field of view will be initially set to be 45° , and will be gradually increased up to 80° , and the phi and theta measures will be obtained for each of size of the field of view. These angular measures will be used in the calculation of the Array Factor and Gain of the antenna.

4.3.2.3 Visualization

In order to obtain both graphics and 2D/3D views of the satellites, sensors, constellations, range and angular measures, we will use a number of options offered by FreeFlyer. Through the *Report* command we will obtain the values of the distance and angular measures. The *Plot* command will illustrate any parameter in relation to another, like the number of satellites that are being included in the field of view depending on the size of the sensor. It can also be displayed in Polar coordinates thanks to the *PolarPlot*. For the visualization of satellites, sensors, constellations, range and angular measures the *Map* command will display our created objects (satellites, constellations, sensors) in two dimensions, and the *View* command will display them in three dimensions.

4.4 Simulation in Matlab

Once all the measures have been obtain in FreeFlyer they are imported to Matlab for further calculations. This will be described in several steps in the following sections.

4.4.1 Data Import

To import the range and angular measurements to Matlab we must first export them as a .xls file from FreeFlyer, and then import them to Matlab as .mat files, to be then stored in array elements. This will be done through the *load* command. We import the range data as a .xls file named *OneWebinter* and then save it as a .mat file named *range*.

4.4.2 Link Budget

Once the data is imported it is necessary to set the link parameters, as the frequency of transmission, temperature of the receiver for the G/T estimation, or the gain that the antenna offers in both the transmitter and receiver. As this project is intended to explore the performance of millimeter waves in ISLs we have chosen the 60GHz frequency band for the OneWeb scenario that we will be simulating. It is important to highlight that we are only taking the OneWeb constellation model for this studio, we are not using its frequency bands for the link budget estimation.

4.4.2.1 Array antenna design

For this project a planar phased array antenna with uniform feed has been selected. A total of 4 array antennas would be placed as it is shown in Figure 4.5 (in blue) in order to establish the intraorbital (yellow) and interorbital (red) ISLs, two for the intraorbital ISLs and two for the interorbital ISLs. An array antenna offers some advantages compared with reflectors, which represent an alternative option, specially in LEO satellites, as they tend to offer better options in terms of size (reflectors are normally bigger in size which affects the entire payload). The other main advantage is that arrays have the ability to rapidly switch direction thanks to multi beam techniques [13]. A simple scheme of the array is shown in Figure 4.4.

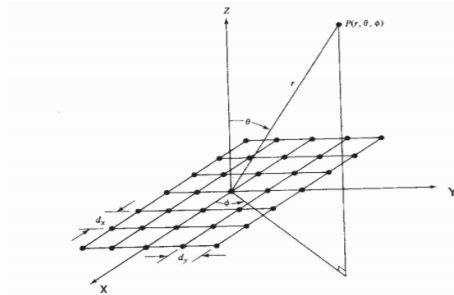


Figure 4.4 Rectangular array antenna [14]

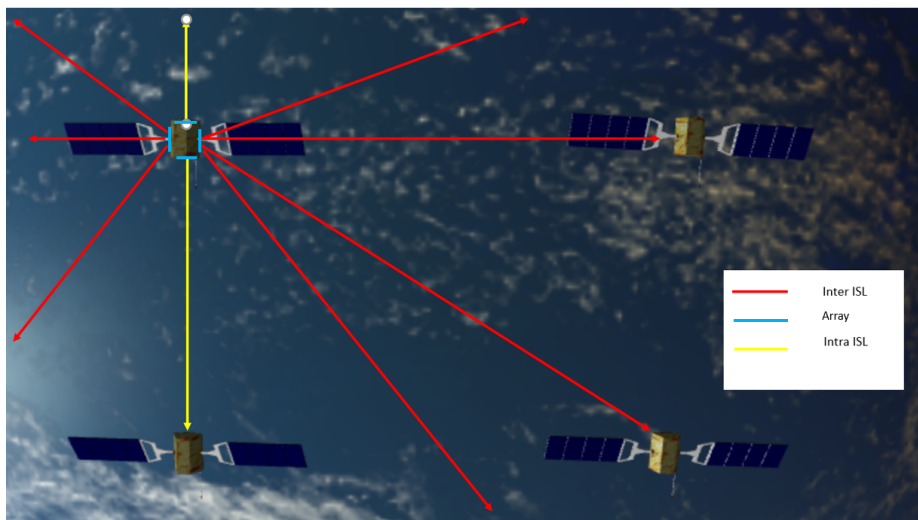


Figure 4.5 Array placement

Using the angular measures of theta and phi that were imported from FreeFlyer, the maximum value of both will be taken for the calculation of the Array Factor carrier frequency

(60GHz) described in Equation 4.3 as part of the wavenumber parameters Ψ_x (for the N row elements) and Ψ_y (for the M column elements) that are described in Equations 4.1 and 4.2.

$$\Psi_x = \frac{2\pi}{\lambda} d_x \sin(\theta) \cos(\phi) + \alpha_x; \quad (4.1)$$

$$\Psi_y = \frac{2\pi}{\lambda} d_y \sin(\theta) \sin(\phi) + \alpha_y; \quad (4.2)$$

$$AF = \left| \frac{\sin(N(\Psi_x/2))}{(\sin(\Psi_x/2))} \right| \left| \frac{\sin(M(\Psi_y/2))}{\sin(\Psi_y/2)} \right| \quad (4.3)$$

The α_x and α_y parameters, as it is shown in Equations 4.4 and 4.5, refer to the constant phase shift between the different row and column elements of the array. For the elements of the array we have assumed a distance between elements (d_x and d_y) of $\lambda/2$.

$$\alpha_x = -\pi \sin(\theta) \quad (4.4)$$

$$\alpha_y = -\pi \sin(\theta) \quad (4.5)$$

We take the maximum *theta* and *phi* values (those are the angular values from the neighbour satellites that are located within the field of view) in order to obtain the gain value for the antenna in a worst case scenario, this is, when it is pointing at the edge of the field of view. For the elements of the array we have assumed to have rectangular patch antennas, which typically present a maximum gain value of 7-8 dB (*Max.G*) and an efficiency (η) of 0.7. Through Equation 4.6 we can obtain the *theta* angle for our radiation pattern where the gain value has fallen 3dB. Then, assuming that the radiation pattern can be approximated by a cosine raised to a certain constant factor (q), we can obtain that q factor by using the *theta* value that we just calculated. By knowing the q factor we will be able to estimate the gain fall for any *theta* from the radiation pattern of the element. The gain value of our interest will be for the maximum *theta* that has been imported to Matlab, as it is shown in Equation 4.7.

$$\theta_{-3dB} (^{\circ}) = \sqrt{\frac{\eta 48360}{10^{\frac{Max.G(dB)}{10}}}} \quad (4.6)$$

$$G_{element}(dB) = Max.G(dB) + 20 \log_{10}(\cos(\theta_{max})^q) \quad (4.7)$$

The radiated field of the antenna is given by Equation 4.8:

$$E_{array} = AF E_{element} \quad (4.8)$$

We will use the $G_{element}$ parameter to obtain the gain of the array antenna and then calculate a CNR value that is within the DVB-S2 MODCOD required values. If it does not meet the standards we will either increase the number of elements of the array in order to increase the gain or increase the output to obtain a better EIRP until the link budget is feasible.

4.4.2.2 System temperature calculation

In order to calculate the G/T parameter the other value we must obtain is the noise temperature in the receiver. To do that we will use the expression shown in Equation 3.2 in the previous chapter. There, T_a is the temperature of the antenna in the receiver, which is set to be typically 20K in the case of ISLs, as it is not pointing to the surface of the Earth (if that was the case the T_a would be 290K). It is significantly low due to the low cosmic sky temperature. The other term, T_{rx} is the equivalent temperature of the modules within the receiver, including the Low Noise Amplifier, the downconverter (with both the local oscillator and the mixer) and the rest of the payload in the receiver. This is shown in Figure 4.6.

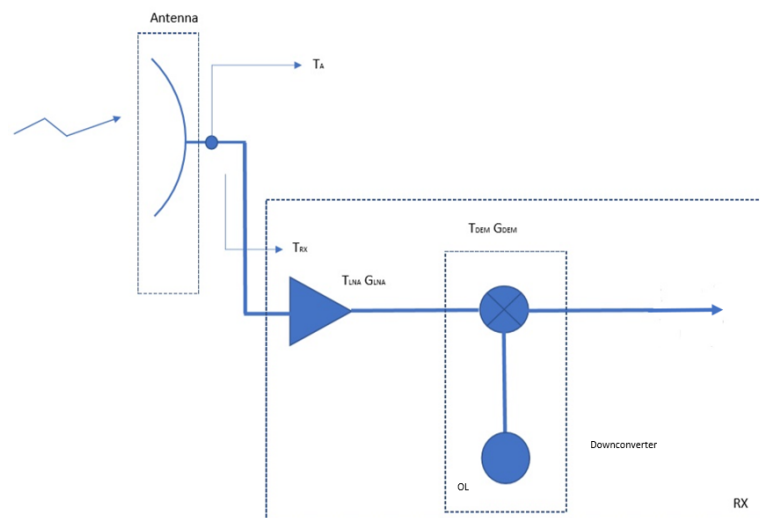


Figure 4.6 Noise temperature at the receiver

There, T_{rx} can be defined as the sum of the noise temperature factors of the different elements that compose the receiver, as it is shown in Equation 4.9:

$$T_{rx} = T_{LNA} + \frac{T_{downconverter}}{G_{LNA}} \quad (4.9)$$

In Chapter 6 a full architecture of both transmitter and receiver will be presented, and based on the results obtained, commercial elements will be selected for the different elements that form them, and the parameters exposed in Equation 4.8 will be specified.

4.4.2.3 Adaptive Coding and Modulation (ACM) and link budget

Once the main parameters in both the transmitter and receiver have been defined we can begin to calculate the link budget. In order to do it an Adaptive Coding and Modulation or link adaptation technique has been used. ACM basically refers to the matching of the modulation, coding and therefore bit rate to the conditions on the radio link. Based on the MODCOD Table (in Appendix C) for the DVB-S2 standard, we will dynamically adapt the modulation and coding schemes. We use the Equation 3.1 to obtain an initial value of the CNR using the first range value imported from FreeFlyer to estimate the free space propagation losses, and using an initial bit rate as Equation 4.10 shows (B stands for bandwidth, which is set to be 10.5 MHz (due to the fact that it was a suitable value for the bit rate standards for an ISL, and DVB-S2 bandwidth restrictions will essentially depend on the services we want to provide), eff stands for spectral efficiency and $\alpha_{roll\ off}$ stands for the roll-off factor which can be 0.2, 0.25 or 0.35 for the DVB-S2 standard).

$$R_b = B \frac{eff}{(1 + \alpha_{roll\ off})} \quad (4.10)$$

Once that value is calculated, it is compared with the MODCOD CNR requirements (adding a security margin M_s) as it is shown in Equation 4.11. All the D values between our single CNR value and the different CNR required values are stored in a *Difference* array. Once this process is completed we search the minimum D value, which will indicate the closest CNR requirement to our CNR value, enabling us to use its modulation and coding scheme. This will make the link budget more efficient as it will change both modulation and coding depending on the link conditions. Therefore, when the ISL distance increases, the link will dynamically adapt to the deterioration of the propagation conditions. A graphical summary of this process is shown in Figure 4.7.

$$D(dB) = CNR - CNR_{required} - M_s \quad (4.11)$$

This strategy will be iterated to calculate the CNR for every range value that was imported from FreeFlyer.

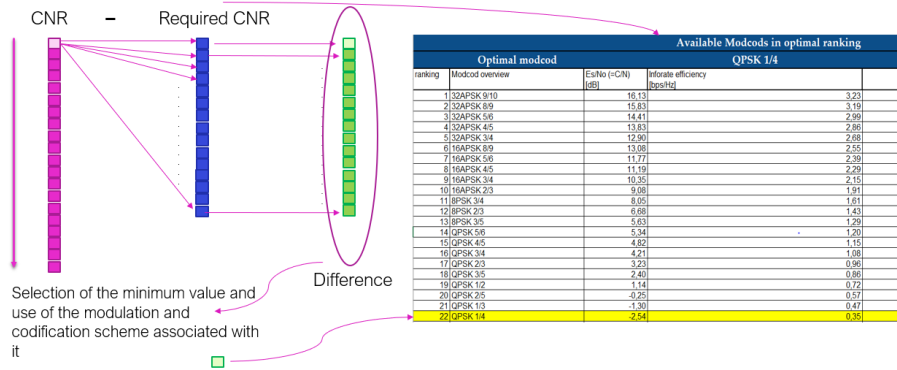


Figure 4.7 ACM scheme

Simulation Results

5.1 Introduction

In this chapter we are going to present and comment the result for the simulation of the selected use case.

5.2 Range

A OneWeb constellation model was implemented in FreeFlyer successfully. For the results of the range measures we obtained reasonable results for both the intraplane and interplane measures. In the case of the intraplane measures we obtain a constant value, as we were using the Two-Body orbital propagator. In the interplane measures we can observe that it has a periodic behaviour, as the satellites will be periodically drifting away and approximating each other. These results are exposed in Figure 5.1 (intraplane measures in blue and interplane measures in red) and in the range Table in Appendix C.

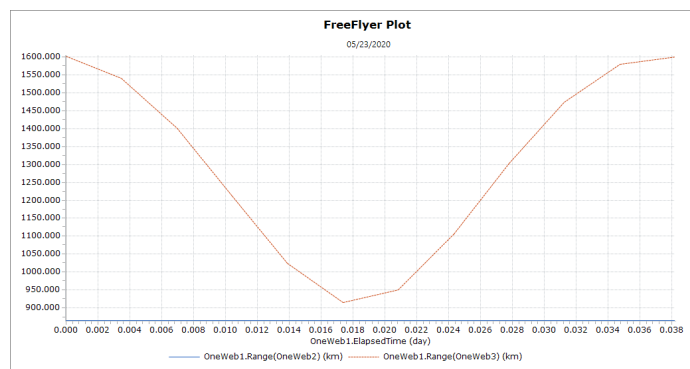


Figure 5.1 Interorbital and intraorbital ISL range graphic in One Web

These range measures have been exported to Matlab for the CNR estimation.

5.3 Angular measurement

The interplane sensor of our analysis was orientated with an Euler-angle FreeFlyer configuration of $\{0^\circ, 270.0^\circ\}$ so that the plane of the antenna would be parallel to the orbital plane (shown in Figure 5.2).

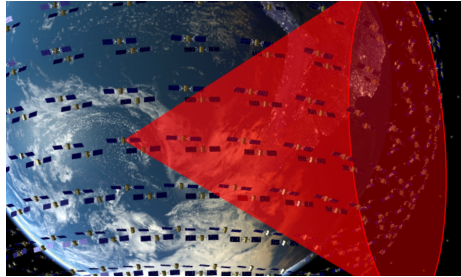


Figure 5.2 Interorbital sensor orientation

The Euler angles $\{\alpha, \beta, \gamma\}$, which define the orientation of the sensor, are defined as in Figure 5.3:

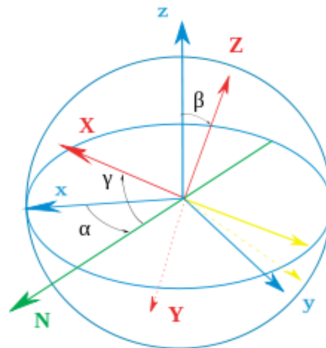


Figure 5.3 Euler angles system

In order to calculate the maximum *theta* and *phi* values we set an initial value of 45° for the field of view of our sensor (cone half-angle). It was gradually increased from this initial value to 80° . Both maximum *theta* and *phi* values were estimated for each field of view angular value. The results are shown in Table 2 and in Figure 5.4.

The Polar representation of the elevation and azimuth angular values for each detected satellite is shown below for the maximum field of view.

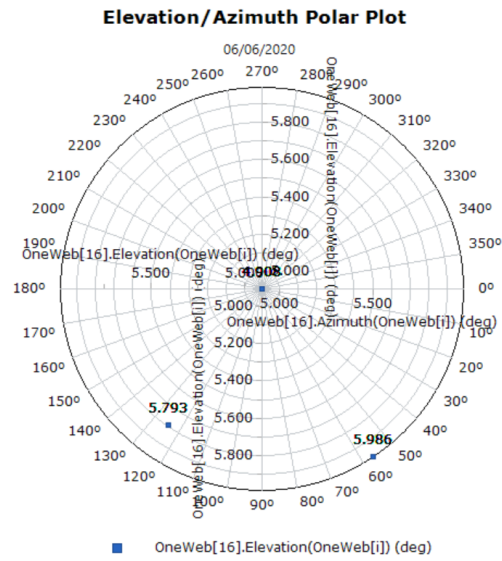


Figure 5.4 Elevation/Azimuth Polar Plot

Max θ , ϕ values and number of visible satellites			
Field of view($^{\circ}$)	θ ($^{\circ}$)	ϕ ($^{\circ}$)	N $^{\circ}$ satellites
45	4.912182141	88.796668037	1
50	4.912182141	88.796668037	1
55	4.912182141	88.796668037	1
60	4.912182141	88.796668037	1
65	4.912182141	88.796668037	1
70	6.038057317	123.642418073	3
75	6.038057317	123.642418073	3
80	6.038057317	123.642418073	3

Table 2 Maximum θ and ϕ values relative to the field of view

When the field of view reaches a value of 80° the sensor is able to have LOS with a total number of 3 satellites. We can observe that θ and ϕ increase as more satellites are detected.

We made the comparison of the number of satellites that we would cover for an interplane ISL if we orientated our sensor in a different direction (Euler angles 0° , 270° , 70°), as it

is shown in Figure 5.5. Here we could encompass a larger number of satellites within our field of view. However the path losses could become a bigger problem as the ISL distances are larger in this particular case. Figure 5.6 shows the elevation/azimuth polar plot for this orientation setting.



Figure 5.5 Alternative sensor orientation

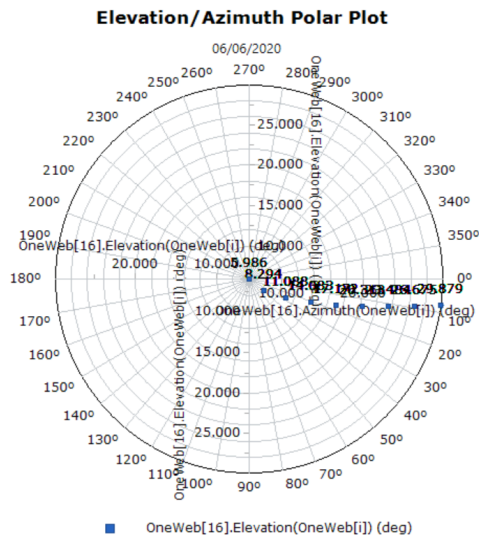


Figure 5.6 Elevation/Azimuth Polar Plot for the new sensor orientation

In the case of the intraplane sensor we followed the same approach. We will only establish an ISL with the adjacent satellite from the orbital plane, therefore we obtain a single value for θ and ϕ of 3.27° and 358° , respectively. The orientation of the sensor is shown in Figure 5.7 below.

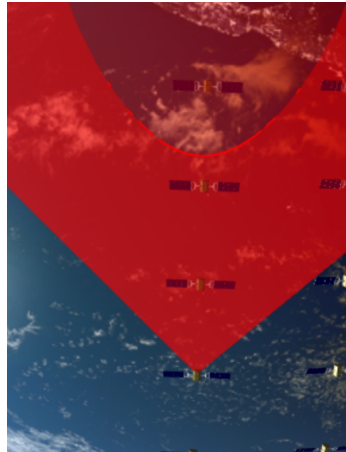


Figure 5.7 Intraorbital sensor orientation

These results are exported to Matlab for the design of the antenna in the intraplane and interplane ISLs (array factor and gain calculation).

5.4 Link Budget

Now the link budget results will be exposed for both the interorbital and intraorbital ISL scenarios. This is, firstly, to illustrate how the array antenna is designed, based on the angular values we obtained previously, and its main characteristics, described in Chapter 4. Then, to show the results for the estimation the CNR and bit rate we performed in Matlab for the range values we calculated previously. As we mentioned, in both cases the ISL will be analysed using the 60GHz frequency, and our range measures will be obtained from a OneWeb constellation model.

5.4.1 Interorbital

In the case of the interorbital ISL the transmitter parameters were set to be $P_{Tx} = 15 \text{ W}$, the gain of the antenna, based on the maximum theta and phi values obtained in the angular measures is set to be 28.0847 dB, following the process described in Chapter 4 Section 4.4.2.1 for the antenna model that we chose, which is an array composed of rectangular patch antennas. Figure 5.8 shows a graphic for the gain fall off depending on the value of *theta* for a single element of the antenna. We can observe that the gain fall value for our angular measures is not significant, compared to the beamwidth at -3dB, which corresponds to a *theta* value 36°.

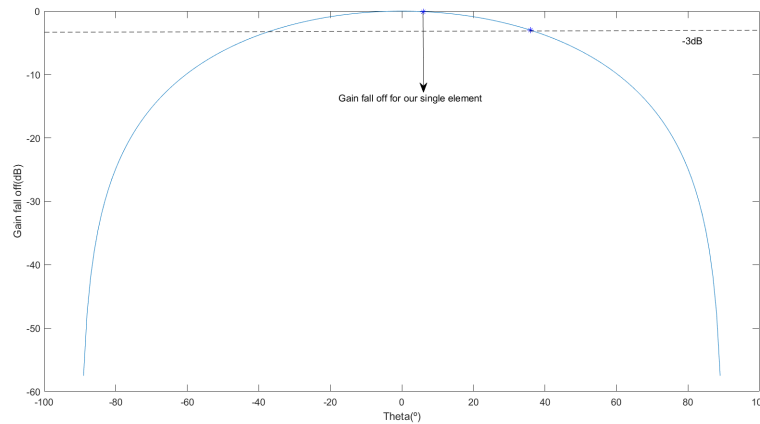


Figure 5.8 Gain fall graphic for a single element of the antenna

As it will be explained later in Chapter 6, the receiver will use a Low Noise Amplifier that will primarily define the noise temperature. Its noise figure is set to be 1.9 dB. This will also determine the link budget outcome as it will define the G/T parameter along with the gain of the antennas. It is worth mentioning that in order to calculate the link budget a compromise between the P_{Tx} and the gain of the antenna must be attended. In order to meet the CNR requirements we can either increase the P_{Tx} or the number of elements in the array to obtain a higher $EIRP$ value. If we increase the P_{Tx} we will not need a large number of elements in the array, therefore the gain will be reduced. This makes the beam of the antenna to be less directive as we establish a loose pointing and tracking configuration. However as the P_{Tx} increases, power dissipation problems will start to appear, therefore this value cannot be increased endlessly. On the other hand, if we increase the number of elements in the antenna we will obtain a higher gain value. However there is also a limit to it as there are size requirements that must be met and antennas should be relatively small. In our case we have chosen a balance between these two parameters.

Therefore the P_{Tx} has been set to be 15 W and the number of elements of the antenna is set as 30x30 elements. This has been done after an iterative process, for which we started calculating the link budget for a P_{Tx} value of 10 W and an array antenna of 4x4 elements. As the CNR requirements were not met we started varying the two elements until we finally obtained 15 W and 30x30 elements. Note that this is the minimum CNR that meets the requirements. We can either increase the P_{Tx} or the number of elements of the array to obtain higher CNR values, but this will require additional costs.

The CNR results meet the requirements, as it is shown in the Figure 5.9. Its values go from 0.1384 dB to 4.9917 dB, which makes our ISL feasible for the selected configuration.

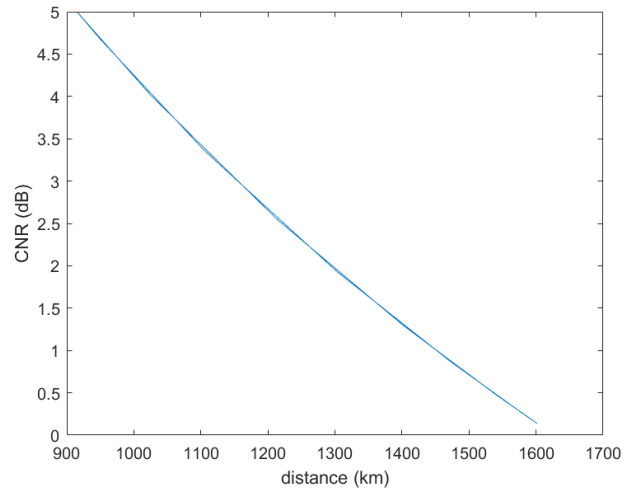


Figure 5.9 Interorbital Range-CNR graphic

Unlike the intraorbital analysis, the interorbital case presents significant range variations which produce an increment in the path losses. The Adaptive Coding and Modulation techniques described in Chapter 4 can be shown as bit rate fluctuations depending on the link conditions. This can be easily seen in Figure 5.10. It shows the bit rate variation depending on time. Its minimum value is of 2.7222 Mbps and its maximum is of 6.6831 Mbps. It is coherent with the ACM techniques, as the bit rate increases as the satellites approximate each other and the path losses are lower (it matches what Figure 5.1 shows in terms of the distance variation).

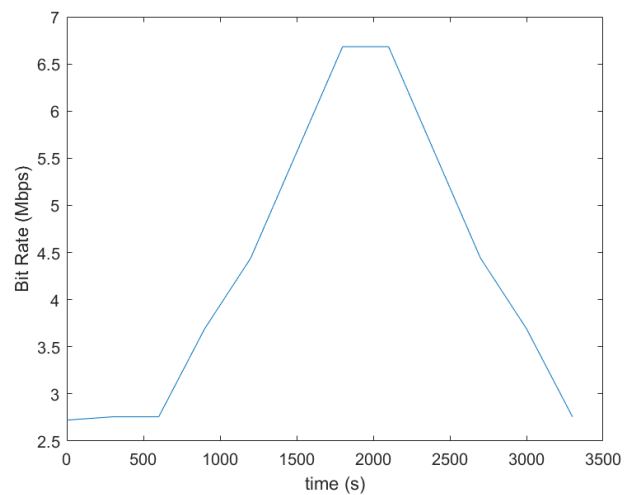


Figure 5.10 Interorbital Time-Bit Rate graphic

Figure 5.11 shows the relation between the path losses and the distance between the

two satellites. They increase as the distance value increments.

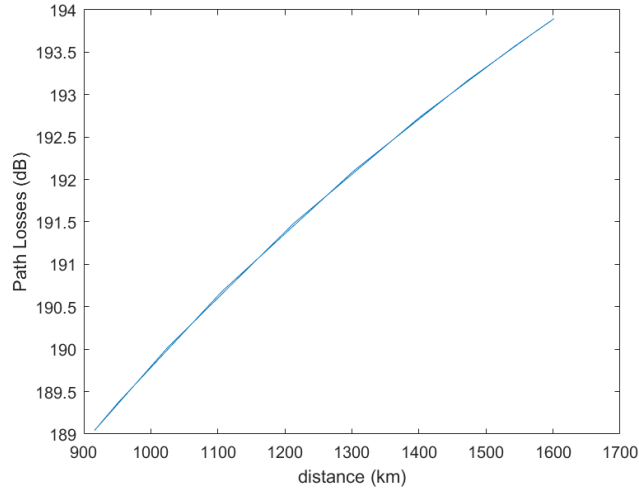


Figure 5.11 Interorbital Range-Path Losses graphic

5.4.2 Intraorbital

For the intraorbital we did not need to set the same P_{Tx} and gain parameters as the distance will remain constant and the ISL will be established between adjacent satellites from a specific orbital plane. Therefore our P_{Tx} was set to be 10 W and the antenna was composed of 9x9 elements, which gave us a gain of 26.5862 dB for our antenna. Through an iterative process in which we gradually increased the number of elements of the antenna, we obtained a CNR value that met the provided requirements.

Based on our calculation a CNR of 0.4797 dB was obtained (this means we are using a MODCOD configuration of a QPSK modulation and $\frac{1}{4}$ coding rate), which is a reasonable value that meets the requirements. Note that this is the minimum CNR that meets the requirements. We can either increase the P_{Tx} or the number of elements of the array to obtain higher CNR values, but this requires additional costs. The path losses have a value of 188.5476 dB. Figure 5.12 shows the bit rate graphic in relation to the time parameter. We can observe that there is an initial adaptation phase until it reaches the 2.722 Mbps. It does not vary from then on as the link conditions do not change significantly.

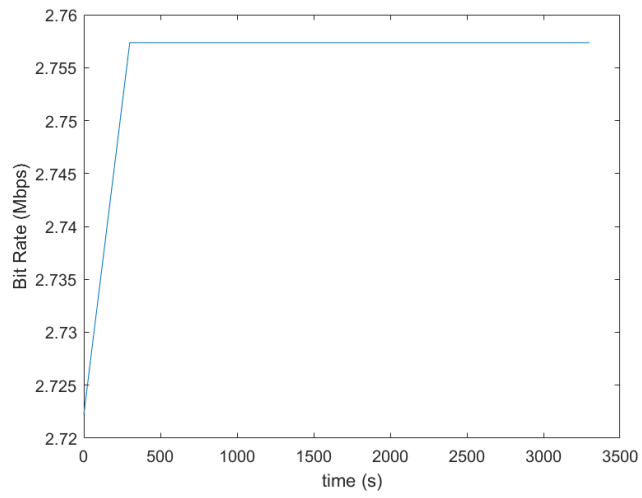


Figure 5.12 Intraorbital Time-Bit Rate graphic

Payload Architecture

6.1 Introduction

In this chapter we are going to describe the architecture and separate modules of the ISL transceiver. Each separate module will be explained in various sections.

6.2 Communication Payload

A complete illustration of the structure of the communication payload is shown in Figure 6.1. The signal could be both received and transmitted to the ground segment in an uplink frequency/downlink frequency, which are located in the Ku band (for the user links) or the Ka band (for the gateway links). Therefore, the transceiver will need to perform up-conversions and down-conversions from the Ku/Ka band to the V band and vice versa, or a Ku/Ka conversion when it directly relays the signal from the user link to the gateway or vice versa. Several Input Multiplexers (IMUX), Output Multiplexers (OMUX) and RF Switches are used to route the signal to the desired transmitter. This architecture provides the satellite with reconfigurability and adaptability properties that can improve its performance. A number of amplifiers will be used at both ends of the ISL to amplify the signal from the OMUX (High Power Amplifier) to the transmitter and from the receiver (Low Noise Amplifier).

Now we will explain in separate sections the architecture of the transceiver, and the particular features of each possible path within the transceiver, as well as the component selection.

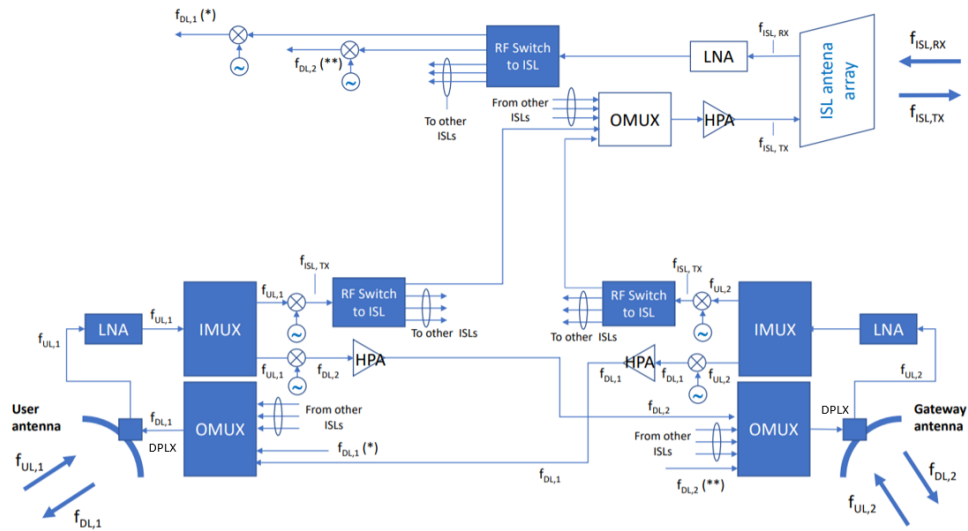


Figure 6.1 Structure of the communication payload

6.2.1 User link - ISL

If the communication payload connects the user link with the ISL the path the signal will follow will be as it is shown in Figure 6.2.

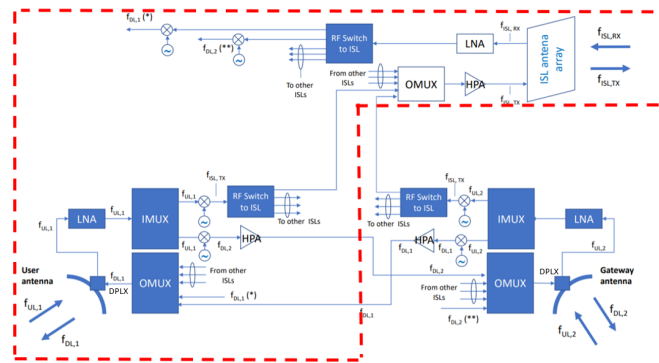


Figure 6.2 User link - ISL architecture

The antenna that is connected to the user link has an integrated diplexer. This diplexer will both route the signal to the ISL transmitter and receive the signal from the ISL receiver. A Low Noise Amplifier will improve the SNR level from the received signal to then send it to a filter bank functioning as an IMUX to decompose the input signal into different output signals that will be routed from the output ports to the different transmitters in the satellite. Then, thanks to a millimeter wave local oscillator and a mixer, an up-conversion will be performed to modulate our signal to the V band.

An RF Switch will be employed to send signals to their respective ISL paths. Then an OMUX will combine all the signals coming from different paths to be then amplified through a High Power Amplifier in order to be sent. Note that our ISL antenna is represented with separate transmission and reception ports, this is due to the fact that array antennas usually employ an input/output interface, and integrate the HPA and LNA modules. Received signals from the ISL pass through a Low Noise Amplifier and then redirected thanks to another RF Switch to the user link antenna. A down-conversion takes place to demodulate the signal from V band to Ku band and then sent to the user link.

6.2.2 Gateway link - ISL

The architecture for the gateway link - ISL path is identical to the user link - ISL path, although the up-conversion/down-conversion would be between the Ka and V band. This is shown in Figure 6.3:

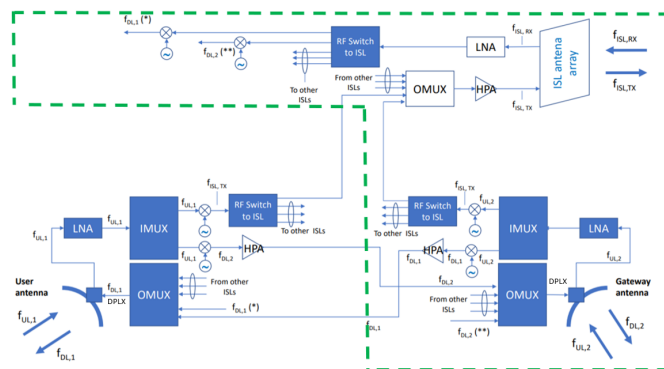


Figure 6.3 Gateway link - ISL architecture

6.2.3 ISL - ISL

In the case of an ISL-ISL relay a frequency conversion from the transmitter to the receiver band will be performed, as they work in separate frequencies. This conversion will be performed before the signal gets to the RF Switch to be redirected to the ISL transmitter. The LNA and the HPA will still be used as well in this scenario. This is shown in Figure 6.4:

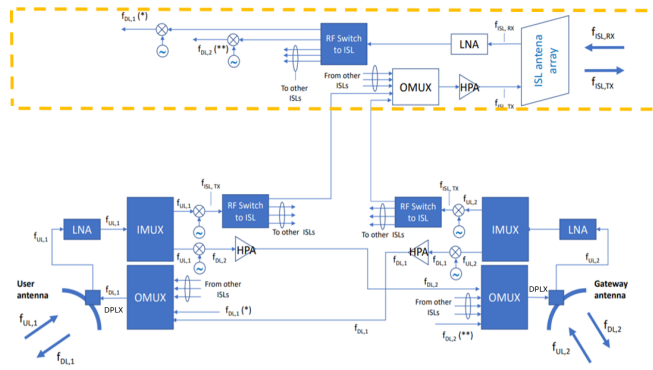


Figure 6.4 ISL - ISL architecture

6.2.4 User link - Gateway link

When the satellite routes the signal in the a user link - gateway link path the architecture is fairly simple. The frequency conversion is either from Ka to Ku or from Ku to Ka. No RF Switch is needed. This is shown in Figure 6.5:

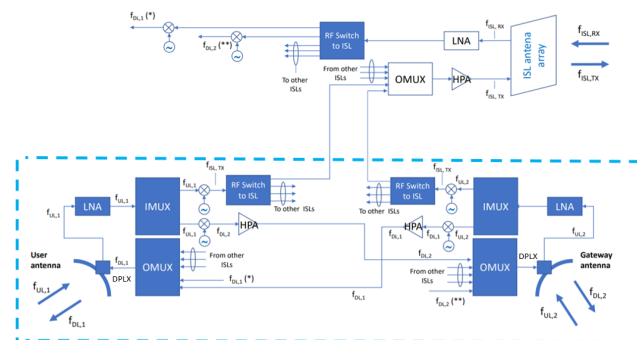


Figure 6.5 User link - Gateway link architecture

6.3 Component selection

Now we will explain the different components of the architecture, giving some commercial references and parameters to those that are specially important for the link budget calculation.

High Power Amplifier:

This kind of amplifiers are used to deliver high output powers amplifying the signal from the satellite in order to be sent through the ISL. There are two main kinds of HPAs

in millimeter wave applications: Traveling wave tube amplifiers (TWTA) and solid-state power amplifiers (SSPA). We will first expose the main characteristics of them both to expose the one that was selected for this specific application.

- *TWTA*: TWT amplifiers are normally more stable over temperature, and they have better heat dissipation capabilities. They offer many years of reliable operation but they have a limited lifetime [16]. Therefore they need to be replaced once this lifespan is exceeded. They have higher power output than SSPA. Currently commercial TWTA models for space applications are not available for frequencies above 50GHz [17].
- *SSPA*: SSP amplifiers are smaller in size than TWTA, which gives a major advantage to SSPA in order to be integrated in LEO satellites. Heat dissipation is one of its most challenging aspects, however SSPAs have better noise power and harmonics capabilities, which is specially useful for LEO ISLs due to the small gain of the antennas. They do not have a limited lifetime[18].

Therefore we have chosen to use a HPA/SSPA amplifier for our transceiver. The ERZ-HPA-5000-6600-19 [15] offered by ERZIA was used as a commercial model for our amplifier. Its main parameters are shown in the Table below:

HPA/SSP Amplifier Datasheet	
Parameter	Value
Type	Solid-State Power Amplifier
Frequency Range(GHz)	50-66
Gain (dB)	22

Table 3 V band HPA/SSPA parameters

The selected model is shown in Figure 6.6:



Figure 6.6 ERZ-HPA-5000-6600-19

Low Noise Amplifier:

LNAs main function as part of the scheme of the receiver is to amplify a very low power signal in a way that the SNR does not deteriorate. Thus, the noise power needs to be controlled so that it is not amplified in the same way as the signal. A low noise figure is therefore important to perform this amplification process. The gain parameter normally needs to be carefully selected. High gain values can amplify greatly the received signals, however it might cause some distortion problems and might generate additional noise.

Currently millimeter wave LNA are normally realized with InP (indium phosphide) high electron mobility transistor (HEMT) or GaAs (gallium arsenide) metamorphic high electron mobility transistor (mHEMT) technology. The InP HEMTs can function as LNAs operating at RF, microwave and millimeter wave frequencies. They present good noise and gain performance. Their cost tends to be high, their production process tends to be unpractical, which makes it hard to produce them in high amount, and they experiment low development. On the other hand, the GaAs LNAs have a lower cost in terms of production when comparing them to the InP HEMTs, and therefore are commercially more appealing for critical applications. It is also easier to produce in large amounts. Along with its better commercial characteristics it has better power handling. The GaAs LNA model is more suitable for this project, as reliability in ISL is a major requirement to be covered. InP HEMTs are more used for scientific research in electrical devices that require very high sensitivity and for less commercial applications. The LNA proposed in [19] serves as a model for our project. It works within our frequency range, including the 60GHz frequency band. The average noise figure is less than 2dB and the linear gain is above 20dB, which meets the LNA performance requirements. It will be the main component from the receiver structure that will determine the noise temperature at the receiver for the estimation of the link budget. Its main parameters are shown in Table 4 below:

Low Noise Amplifier Datasheet	
Parameter	Value
Type	GaAs
Frequency Range(GHz)	59-66
Gain (dB)	22
Noise Figure (dB)	1.9

Table 4 V band Low Noise Amplifier parameters

Up-converter/Down-converter:

The up-converter/down-converter is composed of a local oscillator (LO) and a mixer that will take both the signal from the IMUX and the LO and will produce an RF signal in the V band or from the RF Switch to the OMUX, down-converting the V band signal to Ku/Ka band. For the mixer we looked at a commercial millimeter wave model named SFB-50375308-1519KF-N1 from ERAVANT that served as an example for our architecture. The model is shown in Figure 6.7:

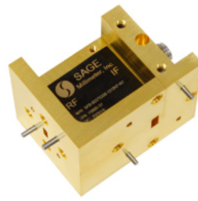


Figure 6.7 SFB-50375308-1519KF-N1

Its main parameter are as follow:

Mixer Datasheet	
Parameter	Value
Type	Balanced
RF Frequency(GHz)	50-75
LO Frequency(GHz)	40-60
IF Frequency(GHz)	DC-35

Table 5 V band Mixer parameters

In the case of the local oscillator it would only be necessary to cover a LO Frequency range that enables the up-converter to modulate the signal from the Ku (12-18 GHz) or Ka band (26.5-40 GHz). Its main parameters would need to be:

Local Oscillator Parameters	
Parameter	Value
Frequency Range(GHz)	35-55
IF Frequency(GHz)	DC-15

Table 6 V band Oscillator parameters

RF Switch:

These are passive RF components of the satellite that can modify the configuration of the payload. A number of control pins route incoming signals through different paths. In our case they will provide configurability for the available ISL in the satellite. We have chose the PE42525 RF Switch model from Peregrine Semiconductor Company, as it is shown in Figure 6.8 [20]:

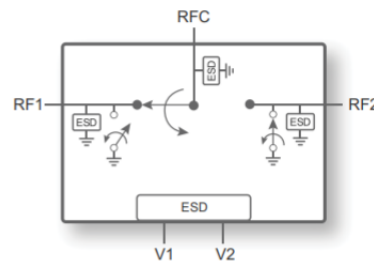


Figure 6.8 PE42525

IMUX/OMUX:

The Input Multiplexer (IMUX) works as a filter bank for incoming signals. It divides them into various channels increasing capacity. Low group delay and high attenuation outside of the selected band are needed to obtain good performance. The Output Multiplexer (OMUX) is employed as a combiner after the HPA to separate signals designated to different beams in a multibeam systems. OMUX need to present low insertion losses to avoid a reduction in the transmitted power level. Spectral dispersion needs to be controlled as well to have a low group delay. Figures 6.9 and 6.10 illustrate a simple example of both:

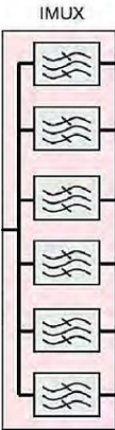


Figure 6.9 IMUX

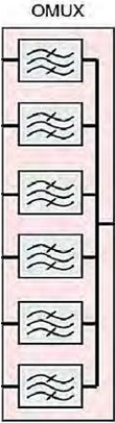


Figure 6.10 OMUX

Conclusions and future work

7.1 Conclusions

After obtaining the results for the simulation in Chapter 5 we concluded that both the graphics and numerical values that we got were reasonable. The CNR values met the requirements of the DVB-S2 MODCOD we used for our link budget configuration and the bit rate values were within the range that was expected.

We can observe that the intraorbital ISL has a higher bit rate throughput and CNR results than the interorbital ISL. The intraorbital ISL makes a more efficient use of the channel capacity (10.5 MHz), providing a data rate of 10 Mbps. Compared to it, the interorbital ISL only reaches approximately 6.5 Mbps. This indicates that it may be reasonable to choose intraorbital ISL over interorbital when planning routing schemes for satellite communications between different ground segment terminals.

In terms of the component selection, the state-of-art of V band components for space application is still in an early development stage. We were not able to find commercial models for all the modules of the communication payload. Other components, like the High Power Amplifier, are present in the market, but only in certain models. As we previously mentioned, commercial TWT amplifiers for space applications are not available for the V band. TWT amplifiers offer higher power output, therefore different choices might be taken once the market offers TWT amplifier that can operate at higher frequency ranges for satellite communications.

Therefore a millimeter wave ISL could be feasible with these parameters. As all the simulations have been performed using the OneWeb constellation orbital parameters, all the measures that were used were inherent to the OneWeb model. Despite of this, the methodology described in Chapter 4 is flexible and can adapt to any other scenario that might be of interest for further analysis.

7.2 Future work

As the methodology of this project is intended to work for other scenarios a similar analysis for different constellation models could be of interest. LEO satellite constellations as Starlink or Telesat are good candidates for this future insight into other LEO uses cases. Other scenarios, as GEO-LEO or GEO-GEO could also be a chosen for further analysis. This will be particularly interesting for millimeter waves in order to test their performances for longer range communication links. We were able to perform similar simulations to the LEO-LEO use case in FreeFlyer to obtain range measures for the Iridium constellation or a GEO-LEO scenario, as it is shown in Figures 7.1 and 7.2. This shows that the path losses and requirements will be completely different for these two uses cases.

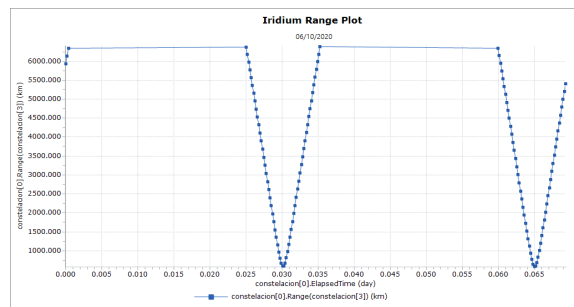


Figure 7.1 Iridium range measures

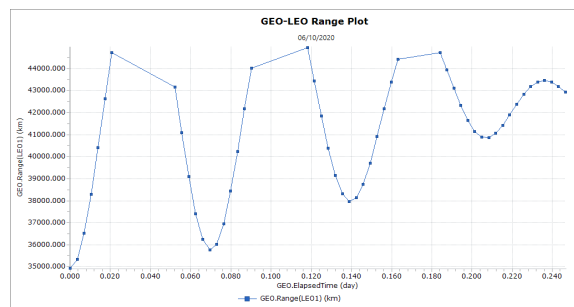


Figure 7.2 GEO-LEO range measures

Apart from that, the interest in optical satellite links is increasing, being a real alternative to millimeter waves to be used for future satellite communications. Optical ISLs offer different characteristics in comparison to millimeter wave ISLs. The size of the antenna at the receiver does not condition the received signal, and they are normally smaller. Optical ISL use lower power compared to millimeter wave ISL [2]. As 5G becomes a reality, and higher data throughput will be highly demanded, optical technologies represent a logic alternative to millimeter wave technologies.

Another significant factor when comparing optical to millimeter wave ISLs is that optical communication systems will typically have a much narrower beamwidth than millimeter systems. This has both a positive and negative side. On one side, a narrower beamwidth reduces potential interferences from or to both adjacent satellites from the same orbital plane or from satellites from the adjacent orbital planes. This is particularly important in massive LEO constellations like OneWeb or Starlink. On the negative side, pointing and tracking requirements will be harder to meet, and it will be more difficult to adapt the spacecraft to these requirements, and it might be a critical factor, as it is critical to the feasibility of optical ISLs. Its state-of-art is not fully developed yet, but it will be a strong contender to millimeter waves in the future for their application to satellite communications.

Another option that might be of interest for future research is combining the two technologies into one single communication system. One could be used for the ISL segment and the other for the uplink and the downlink. There additional losses would need to be taken into account, as the millimeter wave/optical link is no longer established only in space (ISL), but through the atmosphere as well, and consequently oxygen absorption and atmospheric losses will be present.

Outside of satellite communications, there are still multiple applications for millimeter waves that are yet to be fully understood. Chapter 2 briefly looks to five other uses or areas where millimeter waves have been tested. Therefore it might represent a good option for further research.

References

- [1] Campbel, Ashley. December 3, 2018. National American Space Agency (NASA) [Online] Available: https://www.nasa.gov/directorates/heo/scan/communications/outreach/funfacts_text_and_designators.html.
- [2] Fuhrmann, R. S. (1985). Intersatellite link design issues (No. AFIT/CI/NR-86-43T). AIR FORCE INST OF TECH WRIGHT-PATTERSON AFB OH.
- [3] Su, Y., Liu, Y., Zhou, Y., Yuan, J., Cao, H., Shi, J. (2019). Broadband LEO satellite communications: Architectures and key technologies. *IEEE Wireless Communications*, 26(2), 55-61.
- [4] Casey, Kevin. January 31, 2020. The Enterprises Project [Online] Available: <https://enterpriseproject.com/article/2020/1/5g-12-statistics-see>
- [5] Babich, F., Comisso, M., Cuttin, A., Marchese, M., PATRONE, F. (2019). Nanosatellite -5G Integration in the Millimeter Wave Domain: A Full Top-Down Approach. *IEEE Transactions on Mobile Computing*.
- [6] ADUSUMALLI MALLIKHARJUNA RAO, S. K. OVERVIEW OF MILLIMETRE WAVE BAND TO BE USED IN 5G.
- [7] Diederichs, K., Qiu, A., Shaker, G. (2017). Wireless biometric individual identification utilizing millimeter waves. *IEEE Sensors Letters*, 1(1), 1-4.
- [8] Kishore, N., Upadhyay, G., Prakash, A., Tripathi, V. S. (2018). Millimeter Wave Antenna for Intelligent Transportation Systems Application. *Journal of Microwaves, Optoelectronics and Electromagnetic Applications*, 17(1), 171-178.
- [9] Choi, S., Chung, H., Kim, J., Ahn, J., Kim, I. (2016). Mobile Hotspot Network System for High [U+2010] Speed Railway Communications Using Millimeter Waves. *ETRI Journal*, 38(6), 1052-1063.
- [10] ZAMARO, M. (2011). Coupled orbital and attitude SDRE control system for spacecraft formation flying.
- [11] Jones, R. W. (1985). Handbook on Satellite Communications (HSC).
- [12] del Portillo, I., Cameron, B. G., Crawley, E. F. (2019). A technical comparison

of three low earth orbit satellite constellation systems to provide global broadband. *Acta Astronautica*, 159, 123-135.

[13] Sebestyen, G., Fujikawa, S., Galassi, N., Chuchra, A. (2018). *Low Earth Orbit Satellite Design*. Springer International Publishing.

[14] Vakula, D., Sarma, N. V. S. N. (2009). Fault diagnosis of planar antenna arrays using neural networks. *Progress In Electromagnetics Research*, 6, 35-46.

[15] ERZIA Technologies (2016) HPA/SPPA ERZ-HPA-5000-6600-19 Datasheet. <https://www.erzia.com/files/amps/ERZ-HPA-5000-6600-19.pdf>

[16] L3 Communications Electron Technologies, Inc. (2007). *TWT/TWTA Handbook*. <https://www2.l3t.com/edd/pdfs/datasheets/TWT-TWTA%20Handbook.pdf>

[17] Thales Group .Space TWTA Overview. <https://www.thalesgroup.com/en/markets/market-specific-solutions/microwave-imaging-sub-systems/radio-frequency-microwave-sources-4>

[18] Home of RF and Wireless Vendors and Resources. TWTA vs SSPA — Difference between TWTA and SSPA. <https://www.rfwireless-world.com/Terminology/TWTA-vs-SSPA.html>

[19] Longhi, P. E., Pace, L., Colangeli, S., Ciccognani, W., Limiti, E. (2019). Technologies, Design, and Applications of Low-Noise Amplifiers at Millimetre-Wave: State-of-the-Art and Perspectives. *Electronics*, 8(11), 1222.

[20] Peregrine Semiconductor — PE42525 Document Category: Product Specification UltraCMOS® SPDT RF Switch, 9 kHz–60 GHz. <https://www.psemi.com/pdf/datasheets/pe42525ds.pdf>

[21] Global digital population as of April 2020 — Statista. <https://www.statista.com/statistics/617136/digital-population-worldwide/>

[22] 9, Industries, innovation and infrastructure. Sustainable Development Goals. <https://www.un.org/sustainabledevelopment/infrastructure-industrialization/>

Economic budget

A.1 Direct costs

In this section we will expose the direct costs for our project. This is, those costs that are directly associated with the development of the project and the results obtained.

A.1.1 Equipment Costs

For this project we only required the use of a PC for the use of the software tools (FreeFlyer, Matlab, Microsoft Excel, Latex, etc.) and the research associated with the project. The PC that was used was a HP ProBook 430 G5 model that has a total use cost of 700€. The use that was given to this PC for the project corresponds approximately to a 80% of that total cost. This is illustrated in the following table:

Equipment costs	
Model	HP ProBook 430 G5
Use (%)	80%
Cost for a use of 100% (€)	700
Cost for the actual % of use (€)	560

Equipment Costs

A.1.2 License costs

The software tools that were used for the project were essentially four: FreeFlyer (for the simulation of the OneWeb scenario), Matlab (for the link budget calculation), Excel (for various data calculation before importing them to Matlab from FreeFlyer) and Overleaf-

Latex (for the elaboration of the document). The use of Overleaf does not require any installation and is completely free and online. AI Solutions provided us with a FreeFlyer University license which allowed us to make full use of the tool completely free. Therefore the only two software programs that influence the estimation of the licence costs are Matlab (800€) and Microsoft Excel, which is included in the Microsoft Office pack (299€). This is illustrated in the following table:

License costs		
Program	Matlab	Microsoft Office
Annual cost (€)	800	299

License Costs

A.1.3 Labour costs

For the labour costs we take into account the total number of hours that were employed in the development of this project. This includes learning to use the FreeFlyer tool, doing a research for the state-of-art of the topic that the project discusses, programming the scripts in FreeFlyer and Matlab to develop the simulations, executing the simulation scripts and obtaining and analyse the results, writing the final document for the project and elaborating a presentation. We assume an average cost of 20€/hour. This is illustrated in the following table:

Labour costs		
Concept	Number of hours	Cost (€)
Theoretical training	60	1200

FreeFlyer training	50	1000
Matlab development	20	400
FreeFlyer development	60	1200
Results analysis	40	800
Document elaboration	100	2000
Presentation elaboration	20	400
TOTAL	312	7000

Labour Costs

A.2 Project budget

To the direct costs we have to add the indirect costs, that are not directly associated with any specific cost object. These are considered to be approximately the 15% of the direct costs. Added to that is the value-added tax, which is the 21% of the total cost.

Project budget	
Direct Costs: Equipment + License + Labour(€)	8659
Indirect costs (15% of the direct costs) (€)	1298.85
Industrial benefit (6% of the direct costs) (€)	597.47
Total budget without value-added taxation(€)	10555.32
Value-added tax (21%)(€)	2216.62
Total budget(€)	12771.94

Project budget

Therefore the total budget of the project is 12771.94€.

Impact of this project

B.1 Impact

Globalization has been closely related to the impact that the Internet world has had in millions of people. It is estimated that Internet has around 4.57 billion active users [21] and it is obviously expected to have more users every year. The arrival of disruptive technologies like 5G or IoT will help to increase this demand for even faster, better Internet services.

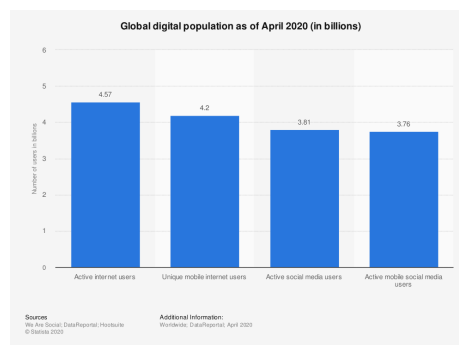


Figure B.1 Global digital population 2020

Therefore it is more urgent than ever to make telecommunication systems and services more accessible globally, to ensure the right to access Internet to make use of those systems and services. However there are still many places that are not able to access Internet completely, and therefore remain isolated from the rest of the world.

It is stated in the Sustainable Development Goals that the access to information and to the Internet must be a fundamental goal to achieve in the near future, in order to reduce the "digital divide". Specially in 9.c where it states that: "Significantly increase the access to information and communications technology and strive to provide universal and affordable access to the Internet in least developed countries by 2020"[22]

On the other hand, Internet helps people to have access to a better education and

information resources. This can help to achieve the tenth goal, which is to reduce inequality among and within countries.

The use of massive LEO constellations like OneWeb or Starlink, that are able to provide services globally achieving large coverage areas and serve as an access point to Internet for isolated areas will play a major role in the process to achieve the Sustainable Development Goals agenda for 2030. The use of massive LEO constellations is also associated with smaller satellites like cubesats. This will make great impact in the manufacturing process of new space communication infrastructure, reducing cost and time. The purpose of this project is to look at the millimeter wave technology as an alternative for this massive LEO constellation models, and how it can help satellite communication to achieve higher data rates and better services by using ISL in the near future.

Tables

DVB-S2 MODCOD				
Ranking	Modulation	Req. CNR (dB)	Code	Efficiency (bps/Hz)
1	32APSK	16.13	9/10	3.23
2	32APSK	15.83	8/9	3.19
3	32APSK	14.41	5/6	2.99
4	32APSK	13.83	4/5	2.86
5	32APSK	12.9	3/4	2.68
6	16APSK	13.08	8/9	2.55
7	16APSK	11.77	5/6	2.39
8	16APSK	11.19	4/5	2.29
9	16APSK	10.35	3/4	2.15
10	16APSK	9.08	2/3	1.91
11	8PSK	8.05	3/4	1.61

12	8PSK	6.68	2/3	1.43
13	8PSK	5.63	3/5	1.29
14	QPSK	5.34	5/6	1.2
15	QPSK	4.82	4/5	1.15
16	QPSK	4.21	3/4	1.08
17	QPSK	3.23	2/3	0.96
18	QPSK	2.4	3/5	0.86
19	QPSK	1.14	1/2	0.72
20	QPSK	-0.25	2/5	0.57
21	QPSK	-1.3	1/3	0.47
22	QPSK	-2.54	1/4	0.35

DVB-S2 MODCOD

Range measures	
Interplante(km)	Intraplane(km)
1601.7	865.25
1540.3	865.25
1401.4	865.25
1212.7	865.25
1025.1	865.25
916	865.25
950.5	865.25
1106	865.25
1302.3	865.25
1578.9	865.25
1600.5	865.25

Range

FreeFlyer Code

D.1 User guide

D.1.1 Creating a constellation

```
OneWeb.Count = 1980;
  For i = 0 to 35;
    For t=0 to 54;
      OneWeb[t+ i*55].A = 1200 + 6371;
      OneWeb[t+ i*55].I = 86.4;
      OneWeb[t+ i*55].RAAN = 360*(i/36);
      OneWeb[t+ i*55].W = 360*(t/55) + ((360/55)/36)*i;
    End;
  End;
```

D.1.2 Propagating a satellite object

```
While (myFormation[0].ElapsedTime < TIMESPAN(1 days));
  Step Spacecraft1 to (Spacecraft1.Epoch == TIMESPAN(1 days));
End;
```

D.1.3 Propagating a satellite in relation to another

```
While (myFormation[0].ElapsedTime < TIMESPAN(1 days));
```

```
    Step Spacecraft2 to (Spacecraft2.Epoch == Spacecraft1.Epoch);  
End;
```

D.1.4 Configuring a sensor

```
OneWeb.ViewAsGroup = 0;  
OneWeb[0].AddSensor("sensor1");  
OneWeb[0].Sensors[0].Color = ColorTools.Red;  
OneWeb[0].Sensors[0].ConeHalfAngle = 22.5;  
OneWeb[0].Sensors[0].ZAxisAzimuth = 90;  
OneWeb[0].Sensors[0].ZAxisElevation = 60;
```

D.1.5 Calculating range

```
constellation[0].Range(constellation[1]);
```

D.1.6 Creating a VisibilitySegment

```
VisibilitySegment Segment;  
Segment.SetObserver(constellation[0]);  
Segment.SetTarget(constellation[1]);  
Segment.AddOccultingBody(Earth);  
Segment.CelestialObjectOccultationModel = 0;  
If(Segment.Visibility(constellation[0].Epoch) == 1);  
    constellation[0].Range(constellation[1]);  
End;
```


D.2 Range Measures

1	While (OneWeb1.ElapsedTime < TIMESPAN(1 hours));	
2	View OneWeb1, OneWeb2, OneWeb3;	
3	Map OneWeb1, OneWeb2, OneWeb3;	
4	FreeForm: FreeForm	
5	Step OneWeb1;	
6	Step OneWeb2 to (OneWeb2.Epoch == OneWeb1.Epoch);	
7	Step OneWeb3 to (OneWeb3.Epoch == OneWeb1.Epoch);	
8	End;	

1	Report OneWeb1.Range (OneWeb2);
2	Report OneWeb1.Range (OneWeb3);
3	Plot OneWeb1.ElapsedTime, OneWeb1.Range (OneWeb2), OneWeb1.Range (OneWeb3);

D.3 Angular Measures

1	OneWeb.Count = 110;
2	Variable i;
3	Variable j = 0;
4	Variable k = 0;
5	Variable x;
6	List<VisibilitySegment> segmentol[OneWeb.Count];
7	Array Pl;
8	Array Tl;
9	Array viewed;
10	Variable numsatl;
11	
12	
13	
14	For i = 0 to OneWeb.Count-1;
15	OneWeb[i].A = 1200 + 6371;
16	OneWeb[i].I = 87.9;
17	If(i == 0);
18	OneWeb[i].RAAN = 0;
19	ElseIf(i%2 == 0);
20	OneWeb[i].RAAN = 0;
21	Else;
22	OneWeb[i].RAAN = 10;
23	End;
24	If(i%2 == 0 or i == 0);
25	OneWeb[i].W = (360/55)*i;
26	Else;
27	OneWeb[i].W = (360/55)*i - 0.18;
28	End;
29	
30	End;
31	

```

32 OneWeb.ViewAsGroup = 0;
33 OneWeb[16].AddSensor("sensor1");
34 OneWeb[16].Sensors[0].Color = ColorTools.Red;
35 OneWeb[16].Sensors[0].ConeHalfAngle = 22.5;
36 OneWeb[16].Sensors[0].BoresightRotationSeq = {3, 1, 2};
37 OneWeb[16].Sensors[0].BoresightAngles = {0, 270, 0};
38
39
40
41
42
43 While(OneWeb[16].Sensors[0].ConeHalfAngle <= 40);
44
45
46     j = 0;
47
48     For i = 0 to OneWeb.Count-1;
49     If (i != 16) then;
50         segmentol[i].SetObserver(OneWeb[16].Sensors[0]);
51         segmentol[i].SetTarget(OneWeb[i]);
52         segmentol[i].AddOccultingBody(Earth);
53     End;
54 End;
55
56
57
58 For i = 0 to OneWeb.Count-1;
59 If (i != 16) then;
60     If(segmentol[i].Visibility(OneWeb[16].Epoch) == 1 and OneWeb[i].RAAN == 10);
61
62         OneWeb[i].Color = ColorTools.Yellow;

```

```

63         Report i, OneWeb[i].RAAN;
64         j++;
65
66     End;
67 End;
68 End;
69
70
71 numsat1 = j;
72 Pl.Clear();
73 Tl.Clear();
74 Pl.Dimension = j;
75 Tl.Dimension = j;
76
77
78
79     j = 0;
80
81
82 For i = 0 to OneWeb.Count-1;
83
84
85
86
87 If (i != 16) then;
88     If(segmentol[i].Visibility(OneWeb[16].Epoch) == 1 and OneWeb[i].RAAN == 10);
89
90         Plot i, OneWeb[16].Elevation(OneWeb[i]);
91
92         Report OneWeb[i].RAAN/i;
93

```

```
95         Pl[j] = OneWeb[16].Azimuth(OneWeb[i]);
96
97         Tl[j] = OneWeb[16].Elevation(OneWeb[i]);
98
99         PolarPlot OneWeb[16].Azimuth(OneWeb[i]), OneWeb[16].Elevation(OneWeb[i]);
100
101
102
103
104
105
106         j++;
107     End;
108
109 End;
110 End;
111
112 If (Pl.Max != -999.00 and Tl.Max != -999.00) then;
113     Report OneWeb[16].ElapsedTime, Pl.Max, Tl.Max;
114 End;
115 Plot OneWeb[16].Sensors[0].ConeHalfAngle, numsat1;
116 Plot OneWeb[16].Sensors[0].ConeHalfAngle, Pl.Max;
117 Plot OneWeb[16].Sensors[0].ConeHalfAngle, Tl.Max;
118
119 OneWeb[16].Sensors[0].ConeHalfAngle = OneWeb[16].Sensors[0].ConeHalfAngle + 0.5;
120 k++;
121
122 View OneWeb;
123 Map OneWeb;
124 Report numsat1;
125
```

Matlab Code

E.1 Link budget code

```
3
4 tiempo = 0:300:3300;
5 caso = "OneWeb inter";
6
7
8 if( caso == "OneWeb inter")
9     num1 = xlsread('OneWeb_inter.xls');
10    save distancias.mat num1
11    load distancias.mat;
12 elseif( caso == "OneWeb intra")
13    num1 = xlsread('OneWeb_intra.xls');
14    save distancias.mat num1
15    load distancias.mat;
16 end
17
18 d = num1;
19
20 %%
21
22 num2 = xlsread('MODCOD.xls')
23 save modcod.mat num2
24
25 load modcod.mat;
26
27 modcod = num2;
28
```

E.1. LINK BUDGET CODE

```
30
31
32 - for i = 1:length(modcod)
33 -     C_N_req(i) = modcod (i,3)
34 - end
35
36
37
38
39
40
41
42
43 - if ( caso == "OneWeb inter")
44 -     f = 60e+9;
45 -     c = 3e+8;
46 -     q = 1.635;
47 -     Horizontal =30;
48 -     Vertical = 30;
49 -     lambda = c/f;
50 -     theta = 6.038*pi/180;
51 -     phi = 123.64*pi/180;
52 -     dx = lambda/2;
53 -     dy = dx;
54 -     alfax = -pi*sin(theta)
55 -     alfay = -pi*sin(theta)

```

```
57 -     fiy = (2*pi/lambda)*dy*sin(theta)*sin(phi)+alfay;
58 -     FA = (abs((sin(Horizontal*(fiy/2)))/(sin(fiy/2))))*abs((sin(Vertical*(fiy/2)))/(sin(fiy/2))));
59 -     D = (4*pi*dx*dy)/((lambda)^2*cos(theta));
60 -     G = 8 + 20*log10(cos(theta)^2*cos(q));
61 -     Garray = 10^(G/10)*(FA);
62 -     Gt = 10*log10(Garray);
63 -     n = 0.7;
64 -     lambda = 3e+8/f;
65 -     lbf=4*pi.*d./lambda.^2;
66 -     Lbf = 20.*log10(4*pi.*d./lambda) ;
67 -     L = Lbf + 1.8;
68 -     Ptx = 15;
69 -     Gtx = Gt;
70 -     gtx = 10^(Gtx/10);
71 -     Grx = Gt;
72 -     Ta = 10;
73 -     Lfrx = 1;
74 -     lfrx = 10^(Lfrx/10);
75 -     Tf = 300;
76 -     Terx = 3000;
77 -     PIRE = 10*log10(Ptx * gtx);
78 -     Mar = 2;
79
80
81 -     t = Ta + ((10^0.19)-1)*290;
82 -     T = 10*log10(t);

```

E.1. LINK BUDGET CODE

```
84 - k = 1.380648 * 10e-23;
85 - roll_off = 0.35;
86 - B = 10.5e+6;
87 - N = 2;
88 - eff = 0.35;
89 - elseif(caso == "OneWeb intra")
90
91 - f = 60e+9;
92 - c = 3e+8;
93 - q = 1.635;
94 - Horizontal = 9;
95 - Vertical = 9;
96 - lambda = c/f;
97 - theta = 3.27*pi/180;
98 - phi = 359.9999*pi/180;
99 - dx = lambda/2;
100 - dy = dx;
101 - alfax = -pi*sin(theta)
102 - alfay = -pi*sin(theta)
103 - fix = (2*pi/lambda)*dx*sin(theta)*cos(phi)+alfax;
104 - fiy = (2*pi/lambda)*dy*sin(theta)*sin(phi)+alfay;
105 - FA = (abs(sin(Horizontal*(fix/2)))/(sin(fix/2)))*abs((sin(Vertical*(fiy/2)))/(sin(fiy/2))));
106 - D = (4*pi*dx*dy)/((lambda)^2*cos(theta));
107 - G = 8 + 20*log10(cos(theta)^q);
108 - Garray = 10^(G/10)*(FA);
109 - Gt = 10*log10(Garray);
```

```
110 - n = 0.7;
111 - lambda = 3e+8/f;
112 - lbf=4*pi.*d./lambda.^2;
113 - Lbf = 20.*log10(4*pi.*d./lambda) ;
114 - L = Lbf + 1.8;
115 - Ptx = 10;
116 - Gtx = Gt;
117 - gtx = 10^(Gtx/10);
118 - Grx = Gt;
119 - grx = 10^(Grx/10);
120 - Ta = 20;
121 - Lfrx = 1;
122 - lfrx = 10^(Lfrx/10);
123 - PIRE = 10*log10(Ptx * gtx);
124 - Mar = 2;
125
126
127 - t = Ta + ((10^0.19)-1)*290;
128 - T = 10*log10(t);
129
130 - k = 1.380648 * 10e-23;
131 - roll_off = 0.35;
132 - B = 10.5e+6;
133 - N = 2;
134 - eff = 0.35;
135 - end
```

E.1. LINK BUDGET CODE

```
139 - for i = 1:length(d)
140 -
141 -
142 -     Rb = B * eff / ( 1 + roll_off);
143 -     C_N(i) = PIRE + Grx - L(i) -10*log10(k*B) - T;
144 -     c_n_analizada = C_N(i);
145 -     for j = 1:length(C_N_req)
146 -         c_n_limite = C_N_req(j)
147 -         if(C_N(i) > C_N_req(j)+ Mar)
148 -             dif(j) = C_N(i) - C_N_req(j) - Mar;
149 -         else
150 -             dif(j) = NaN;
151 -         end
152 -     end
153 -
154 -     [M,I] = min(dif);
155 -     N = modcod(I, 1);
156 -     eff = modcod(I, 4);
157 -     cod(i) = eff;
158 -     cmod(i) = N;
159 -
160 -
161 -     if(C_N(i) < -2.54 + 2)
162 -         C_N(i) = -Inf;
163 -     else
164 -         C_N(i) = PIRE + Grx - L(i) -10*log10(k*B) - T;
```

```
165 -         c_n_analizada = C_N(i)
166 -     end
167 -
168 -     BW(i) = Rb;
169 - end
170 -
171 -
172 - set(gcf, 'color', 'w');
173 -
174 - plot(d/1000, C_N);
175 - xlabel('distance (km)')
176 - ylabel('CNR (dB)')
177 -
178 - plot(tiempo, BW/1e+6);
179 - xlabel('time (s)')
180 - ylabel('Bit Rate (Mbps)')
181 -
182 - plot(d, C_N)
183 - hold on
184 - plot(d, L)
185 - xlabel('distance (km)')
186 - ylabel('Path Losses/CNR (dB)')
187 -
188 - hold off
189 - plot(d/1000, L)
190 - xlabel('distance (km)')
```